

The Top Quark¹

EDUARD BOOS¹, OLEG BRANDT², DMITRI DENISOV³, SERGEY DENISOV⁴, and
PAUL GRANNIS⁵

¹ Skobeltsyn Institute of Nuclear Physics, Lomonosov Moscow State University, 119992
Moscow, Russian Federation
(e-mail: boos@theory.sinp.msu.ru; Eduard.Boos@cern.ch)

² Kirchhoff Institute for Physics, Heidelberg University, 69120 Heidelberg, Germany
(e-mail: obrandt@kip.uni-heidelberg.de)

³ Fermi National Accelerator Laboratory, Batavia Illinois 60510, USA
(e-mail: denisovd@fnal.gov)

⁴ State Research Center of Russian Federation “Institute for High Energy Physics” of
National Research Center “Kurchatov Institute”, Nauki sq. 1, Protvino, Moscow
region 142281, Russian Federation
(e-mail: denisov@ihep.ru)

⁵ State University of New York, Stony Brook, New York 11794, USA
(e-mail: pgrannis@sunysb.edu)

Abstract

On the twentieth anniversary of the observation of the top quark, we trace our understanding of this heaviest of all known particles from the prediction of its existence, through the searches and discovery, to the current knowledge of its production mechanisms and properties. We also discuss the central role of the top quark in the Standard Model and the windows that it opens for seeking new physics beyond the Standard Model.

1 Introduction

Twenty years have passed since the discovery of the heaviest elementary particle, the top quark, at the CDF and D0 Tevatron experiments [1, 2]. The top quark, being even heavier than the Higgs boson recently discovered at the LHC, remains one of the most interesting objects in the elementary particle zoo.

¹FERMILAB-PUB-15-416-E, Published in Phys. Usp. **185**, 1241 (2015),
[DOI:10.3367/UFNe.0185.201512a.1241](https://doi.org/10.3367/UFNe.0185.201512a.1241).

In 1964 Gell-Mann and Zweig [3, 4] proposed the quark model to explain the experimental observations in accelerator and cosmic ray experiments of many new strongly interacting particles called hadrons. Originally it was enough to introduce only three quarks u (up), d (down), and s (strange) to correctly describe the charges and spins of observed hadrons. In this model, all the quarks are fermions with spin $1/2$ and should have fractional electric charges of $2/3$ (in units of the electron charge) for the u -quark and $-1/3$ for the d - and s -quarks. The proton and the neutron are formed from the quark combinations uud and ddu respectively. The masses of the quarks are a few MeV for u - and d - quarks and ~ 100 MeV for the s -quark, based on measured masses of the proton, neutron, π and K -mesons, and subsequently on deep inelastic scattering measurements. In 1974 a new meson called J/ψ was observed [5, 6] which was quickly interpreted as a bound state of a new quark, c (charm), and its antiparticle, with electric charges $\pm 2/3$. The charm quark had been predicted theoretically to explain the decay properties of charged and neutral K -mesons through the Glashow–Iliopoulos–Maiani (GIM) mechanism [7]. By that time four electrically and weakly interacting particles (electron, electron neutrino, muon, and muon neutrino) were also known, and an interesting symmetric picture appeared containing four quarks, combined into two generations (u, d) and (c, s), and four leptons similarly arrayed in the corresponding (ν_e, e) and (ν_μ, μ) generations. In the mid-1970s this symmetry was broken when the τ lepton was discovered [8] and a new quark, b (bottom), with a mass of about 5 GeV and electric charge $-1/3$ was added to the quark family. The b -quark was inferred from the discovery of the Υ meson at Fermilab [9] at about 10 GeV which was seen to be a bound state of b and \bar{b} quarks. Subsequent measurements at Cornell, DESY and SLAC confirmed this interpretation. If one assumed that the new lepton and quark belong to a third fermion generation, then to recover the quark-lepton symmetry one needed one more quark and one more neutrino to exist. The new ‘top’ quark was discovered in 1995, and in 2000 the tau neutrino was observed in τ -lepton decays in the Fermilab DONUT experiment.

In the Standard Model (SM) the top quark has the same quantum numbers and interactions as all other up-type quarks. It is the weak isospin partner of the b quark with spin $1/2$ and electric charge $Q_{em}^t = +2/3$. The left chiral part of the top quark is the upper component of the weak isospin doublet and the right chiral component is a weak isospin singlet. It is a color triplet with respect to the $SU(3)_c$ gauge group responsible for the strong interactions in the SM. From the theory side, the top quark is absolutely needed to ensure cancellation of the chiral anomaly in the SM and therefore to ensure its consistency as a quantum field theory.

The measured value of the top quark mass at the Tevatron and the LHC is now known with a precision better than 0.5% and is the most precisely determined

quark mass: $m_t = 173.34 \pm 0.27(\text{stat}) \pm 0.71(\text{syst})$ GeV [10]. It is the heaviest known elementary particle, with a mass slightly less than the mass of the gold nucleus and thus does not conform to the original quark conjecture as a simple constituent of hadrons. However, up to now we have no indication of any internal top quark structure; it behaves in all processes as a point-like particle. Two empirical facts distinguish the top from other quarks: its much larger mass and its very small mixing to quarks of the first and second generations. The natural question arises: Why is the top quark so special? Why is it alone in having a mass of approximately the electroweak symmetry breaking scale? In the SM there is no answer to this question.

In another respect the top quark is a unique object. The quark mixing in the SM is encoded in matrix elements of the Cabibbo-Kobayashi-Maskawa (CKM) matrix [11, 12]. The matrix element V_{tb} is close to unity while the elements V_{ts} and V_{td} are significantly smaller than one. These two experimental facts, large mass and small mixing, lead to the conclusion that in the SM the top quark decays to a W boson and b quark with a probability close to 100%. The width of the top is computed in the SM to be about 1.5 GeV [13, 14], much smaller than its mass. On the other hand, the top width is significantly larger than the typical QCD scale $\Lambda \approx 200$ MeV. As a result, the top lifetime ($\tau_t \approx 5 \times 10^{-25}$ s) is much smaller than the typical time for formation of QCD bound state hadrons ($\tau_{\text{QCD}} \approx 1/\Lambda_{\text{QCD}} \approx 3 \times 10^{-24}$ s). Therefore, the top quark decays long before it can hadronize and hence hadrons containing a top quark are not expected to exist [15]. In this respect the physics of the top quark is much simpler than, for example, the physics of B -hadrons, in which bound states of the b -quark with other quarks and anti-quarks form a rich spectroscopy. However, since the top quark decays before hadronization its properties are not hidden by hadronization effects, and therefore it provides a very clean source for fundamental information. In particular, the SM predicts very specific spin correlation properties. Due to the $(V - A)$ structure of the charged currents in the SM, the top and anti-top spins in production are strongly correlated and represent a unique experimental probe in the quark sector through the directions of their decay products.

Two classes of top quark production exist. The first proceeds by the strong QCD force in which a quark and anti-quark or a pair of gluons interact to produce a top and anti-top quark. Since each of the produced tops decays to a W boson and a b quark, the final states are determined by the ways that the W bosons decay. The quarks hadronize in the detector as collimated sprays of hadrons called jets. If both W 's decay to leptons and neutrinos ($\ell\ell$ channel), the final state has two leptons, two (b) jets and missing transverse energy (\cancel{E}_T) carried by the two neutrinos. If one W decays to a lepton and the other to quark pairs (ℓ +jets channel), the final state is one lepton, four jets (of which two are b -jets) and \cancel{E}_T . If both W 's decay to

quarks (all-jets channel), the final state has six quark jets. The second production class proceeds through the weak interaction with a W boson propagator, leading to a single top quark in the final state, associated with at least one other jet.

The top quark, with its large mass and correspondingly large Yukawa coupling $y_t = 2^{3/4}G_F^{1/2}m_t = \sqrt{2}m_t/v$ close to unity, makes a significant impact on various electroweak observables due to SM quantum loop corrections involving top. In particular, the loop corrections to W - and Z -boson masses are proportional to the top mass squared. The fit of precision electroweak data of LEP+SLD by SM computations at loop level allowed the indirect estimate of the top quark mass of $m_t = 177_{-8}^{+7} \text{ }_{-19}^{+17}$ GeV [16] which was in good agreement with the measurements. A modern global fit of precision electroweak measurements by quantum loop corrected SM predictions with a significant top-quark input shows how perfectly SM works as a quantum gauge theory [17].

The loop contribution involving top quarks is one of the most important factors in the Higgs boson self-coupling evolution with energy scale. It is crucial to know the top quark mass value precisely to understand how stable the SM vacuum is. The current precision of slightly less than 0.5% seems not yet good enough to get a concrete answer [18].

Due to the large top quark mass, the Higgs boson mass parameter also gets large loop corrections which depend quadratically on the scale of possible new physics. Such a dependence may lead to the so-called “little hierarchy problem” and motivates a possible existence of top quark partners which might be accessible at the LHC. Such partners, if they exist, may give extra loop contributions, thus canceling the strong quadratic behavior and stabilizing the Higgs mass parameter.

In the following sections we discuss various aspects of the top quark in more detail: In Section 2, a history of searches for the top quark at CERN, DESY and KEK is given. The top quark discovery at the Fermilab Tevatron is described in Section 3. In Section 4 we present details of measurements of the top pair production cross-section. In Section 5 we continue with the discovery of single top production and measurements of the electroweak single top cross-section. Due to importance of the top quark mass, its measurement and related problems are discussed in a special Section 6. In Section 7 the top quark properties such as spin, charge, lifetime, the CKM matrix element V_{tb} are presented. The special role of the top quark in the SM, particularly, in assuring the consistency of the Higgs mechanism of spontaneous electroweak symmetry breaking in the SM is discussed in Section 8. In Section 9 the role of the top quark as a possible guide to new physics is reviewed. A short conclusion is given in the final section.

	<p>mass → $\approx 2.3 \text{ MeV}/c^2$</p> <p>charge → $2/3$</p> <p>spin → $1/2$</p> <p>u</p> <p>up</p>	<p>mass → $\approx 1.275 \text{ GeV}/c^2$</p> <p>charge → $2/3$</p> <p>spin → $1/2$</p> <p>c</p> <p>charm</p>	<p>mass → $\approx 173.07 \text{ GeV}/c^2$</p> <p>charge → $2/3$</p> <p>spin → $1/2$</p> <p>t</p> <p>top</p>	<p>mass → 0</p> <p>charge → 0</p> <p>spin → 1</p> <p>g</p> <p>gluon</p>	<p>mass → $\approx 126 \text{ GeV}/c^2$</p> <p>charge → 0</p> <p>spin → 0</p> <p>H</p> <p>Higgs boson</p>
QUARKS	<p>mass → $\approx 4.8 \text{ MeV}/c^2$</p> <p>charge → $-1/3$</p> <p>spin → $1/2$</p> <p>d</p> <p>down</p>	<p>mass → $\approx 95 \text{ MeV}/c^2$</p> <p>charge → $-1/3$</p> <p>spin → $1/2$</p> <p>s</p> <p>strange</p>	<p>mass → $\approx 4.18 \text{ GeV}/c^2$</p> <p>charge → $-1/3$</p> <p>spin → $1/2$</p> <p>b</p> <p>bottom</p>	<p>mass → 0</p> <p>charge → 0</p> <p>spin → 1</p> <p>γ</p> <p>photon</p>	
	<p>mass → $0.511 \text{ MeV}/c^2$</p> <p>charge → -1</p> <p>spin → $1/2$</p> <p>e</p> <p>electron</p>	<p>mass → $105.7 \text{ MeV}/c^2$</p> <p>charge → -1</p> <p>spin → $1/2$</p> <p>μ</p> <p>muon</p>	<p>mass → $1.777 \text{ GeV}/c^2$</p> <p>charge → -1</p> <p>spin → $1/2$</p> <p>τ</p> <p>tau</p>	<p>mass → $91.2 \text{ GeV}/c^2$</p> <p>charge → 0</p> <p>spin → 1</p> <p>Z</p> <p>Z boson</p>	GAUGE BOSONS
LEPTONS	<p>mass → $< 2.2 \text{ eV}/c^2$</p> <p>charge → 0</p> <p>spin → $1/2$</p> <p>ν_e</p> <p>electron neutrino</p>	<p>mass → $< 0.17 \text{ MeV}/c^2$</p> <p>charge → 0</p> <p>spin → $1/2$</p> <p>ν_μ</p> <p>muon neutrino</p>	<p>mass → $< 15.5 \text{ MeV}/c^2$</p> <p>charge → 0</p> <p>spin → $1/2$</p> <p>ν_τ</p> <p>tau neutrino</p>	<p>mass → $80.4 \text{ GeV}/c^2$</p> <p>charge → ± 1</p> <p>spin → 1</p> <p>W</p> <p>W boson</p>	

Figure 1: The Standard Model table of elementary particles. Similar to the chemical periodic table (with substantially more elements), all currently known composite particles are made of quarks and leptons with forces exchanged by the gauge bosons. Each particle has an antiparticle with the same mass and spin, but opposite electric charge. All of the above particles have no observed substructure down to distances of 10^{-18} cm. The Higgs boson provides mass to the elementary particles.

2 History of searches for the top quark

The quark model discussed in the previous section (see Fig. 1) and the development of the Standard Model in the 1970s [19, 20, 21] implied the existence of a top quark, the charge $+2/3$ partner of the bottom quark. The search for this new quark was to last for twenty years.

Using the ratios of the already observed quark masses, some physicists suggested that the top quark might be about three times as heavy as the b quark, and thus expected that the top would appear as a heavy new meson containing a $t\bar{t}$ pair, at a mass around 30 GeV. The electron-positron colliders then under construction raced to capture the prize. By 1984 the PETRA e^+e^- collider at the Deutsches Elektronen-Synchrotron (DESY) in Germany reached a center of mass energy of 46.8 GeV and excluded the existence of the top quark with a mass about half of the total center of mass energy or 23.3 GeV [22, 23, 24]. The e^+e^- collider TRISTAN with energy of 61.4 GeV was built at the High Energy Accelerator Research Organization (KEK) in Japan in 1986 with the main goal of discovering the top quark. By 1990 experiments at TRISTAN excluded the top quark with mass less than 30.2 GeV [25]. Later, the two $e^+e^- Z$ boson factories SLC at SLAC and LEP at CERN started operation, and by about 1990 set a lower limit on m_t at

Year	Collider(s)	Coll. particles	Limit on m_t	References
1984	PETRA (DESY)	e^+e^-	> 23.3 GeV	[22, 23, 24]
1990	TRISTAN (KEK)	e^+e^-	> 30.2 GeV	[25]
1990	SLC (SLAC), LEP (CERN)	e^+e^-	> 45.8 GeV	[26, 27, 28, 29]
1988	Sp \bar{p} S (CERN)	$p\bar{p}$	> 45 GeV	[31]
1990	Sp \bar{p} S (CERN)	$p\bar{p}$	> 69 GeV	[32]
1991	Tevatron (Fermilab)	$p\bar{p}$	> 91 GeV	[33]
1994	Tevatron (Fermilab)	$p\bar{p}$	> 131 GeV	[35]

Table 1: Summary of increasing mass limits of the mass of the top quark m_t through 1980s and early 1990s.

half of the Z boson mass, $m_t \geq 45.8$ GeV [26, 27, 28, 29].

In the early 1980s, the Sp \bar{p} S collider came into operation at CERN with counter-rotating beams of protons and antiprotons colliding with an energy of 540 GeV (later upgraded to 630 GeV). The protons and antiprotons brought their constituent quarks and antiquarks into collision with typical energies of 50 to 100 GeV. Besides the important discoveries of the W and Z bosons, the carriers of the unified electroweak force, the CERN experiments demonstrated another aspect of quarks. Though quarks had continued to elude direct detection, they can be violently scattered in high energy collisions. The high energy quarks emerging from the collision region are subject to the strong interaction, creating additional quark-antiquark pairs from the available collision energy. The quarks and antiquarks so created combine into ordinary hadrons that are seen in the detectors. These hadrons tend to cluster along the direction of the original quark, and are thus recorded as a “jet” of rather collinear particles. Such quark jets, previously sensed at SLAC and DESY, were clearly observed at CERN and became a key ingredient in the next round of the top quark searches.

With the advent of the Sp \bar{p} S, and in 1988 the more powerful 1800 GeV Tevatron collider at Fermilab, the search for the top quark turned to even higher masses. At the large masses now accessible, the $t\bar{t}$ bound state was unlikely to form (as the top quark would decay faster than the time needed for binding the quarks into a bound state) so isolated top quarks were expected. For $m_t < m_W$, the W boson decay into a top quark and a b quark would predominate. A good channel for the search is $W^+ \rightarrow t\bar{b} \rightarrow e^+\nu_e b\bar{b}$ and the charge-conjugate process. The main background is QCD production of W bosons and jets. In 1984 the UA1 experiment at the Sp \bar{p} S reported evidence for an excess of events with an isolated lepton and two jets, characteristic of a 40 GeV top quark [30]. UA1 observed 6 events (3 with electrons and 3 with muons) with an expected background of less than 1 event. In retrospect, background from $b\bar{b}$ production was underestimated and the top quark “observation” was later ruled out [31, 32]. By 1992 the CDF experiment

at Fermilab had extended the limit to $m_t > 91$ GeV [33], thus eliminating the possibility for the $W \rightarrow t\bar{b}$. In 1992, the D0 experiment joined CDF as a long Tevatron run began, culminating with the discovery of the top quark as described in Section 3. Table 1 summarizes the steadily increasing lower limits on m_t through 1980s and early 1990s.

3 Top quark discovery at the Tevatron

In 1988 the search for the top quark was joined by the CDF experiment in the first physics run of the newly commissioned Tevatron $p\bar{p}$ collider [34] operating at 1.8 TeV. Based on the unsuccessful searches for top quark pairs at e^+e^- colliders and at the CERN Sp \bar{p} S seeking top quarks from the decay $W \rightarrow t\bar{b}$, it became increasingly likely that the top quark would have a greater mass than the W boson. By then, the precision measurement of observables in Z boson decay, neutrino scattering, and the mixing of the neutral K^0 and B^0 flavor eigenstates predicted that the top quark mass, m_t , lay in the approximate range $90 < m_t < 160$ GeV, based on the indirect effects of top quark loops in these processes within the context of the SM.

In 1992, CDF reported a new search for top quark pair production [33] in which both top quarks decay to a W boson (real or virtual depending on the top mass) and a b quark. The search used the $\ell\ell$ channel as well as the ℓ +jets channel. In the latter channel, CDF required at least one of the jets to be tagged as a b -jet, identified through the presence of a low p_T (soft) muon from the semileptonic decay of a B hadron. Comparison of the observed yield of events with SM predictions as a function of m_t gave a lower limit of 91 GeV, thus ruling out the possibility that the W boson decays to top quarks and implying that the dominant production mode would be $t\bar{t}$ pair production.

In 1992, the new D0 experiment, with its high resolution calorimetry and large electron and muon acceptance, began operation at the Tevatron, and in 1994 raised the lower limit to 131 GeV [35], now encroaching on the window set indirectly by the precision measurements. For this run CDF added a new silicon microstrip vertex detector close to the beams that permitted the identification of jets containing a b -hadron that travelled a short distance (a few mm) from the production point, providing a powerful tool for recognition of b -quark jets and suppression of background processes from W +jets and QCD multijet production. Although both collaborations were still setting lower limits on m_t , the limits were not much improved as the data samples increased. In the winter of 1992 – 1993, both collaborations recorded striking events that conformed to the profile expected for top quark pair events. Both events were in the $e\mu$ dilepton channel which has low background. The CDF event had one of the two jets tagged by its silicon mi-

crostrip detector (as well as by a soft muon). The D0 event had an electron, muon and \cancel{E}_T , each with at least 100 GeV transverse momentum. These events were very unlikely to have arisen from the expected background processes and heightened the expectation of a top quark discovery.

By early 1994, CDF found more events in 19 fb⁻¹ of data than were predicted by known backgrounds. The publication [36] claimed evidence for the top quark and reported 12 events in the dilepton channel and the ℓ +jets channel with at least one jet tagged as a b -quark jet by the vertex detector or a soft muon within the jet. The probability for the background to fluctuate to the observed yield was 0.26%, too large to claim the result as a discovery, but small enough to interpret the excess as being likely to arise from top quark production. The fitted mass was $m_t = 174 \pm 16$ GeV and the $t\bar{t}$ cross section was estimated to be about 14 pb, a factor of about two larger than expected from theory at the observed m_t value. Shortly afterwards, D0 reported [37] the results of an analysis in which backgrounds were reduced through the use of topological variables that had a comparable expected sensitivity to CDF, but with only 7 observed events and a 7.2% probability for the background to explain the observed yield.

The appearance of events in excess of the background expectation created the anticipation in both collaborations that more data could bring discovery. During a Tevatron shutdown in summer 1994, the accelerator experts discovered that one of the bending magnets in the machine had been rotated around the beam axis. With this fixed, the instantaneous luminosity grew substantially and by early 1995, the data samples had approximately tripled relative to the 1994 evidence results, and both collaborations sensed that they were sufficient to permit the discovery. Both collaborations updated their selection criteria to optimize the sensitivity for a top quark with mass in the 150 – 200 GeV region. Although there were no interactions between the collaborations on their progress, each knew that the other collaboration was getting close and each began a frenetic push to complete the analyses. An agreement was put in place that when either collaboration presented a paper draft to the Fermilab Director, a one week period would start during which the other collaboration could finalize a paper, and if so, a simultaneous submission for publication would occur. CDF delivered its paper in mid-February and one week later, on February 24, 1995 both collaborations submitted their discovery papers to Physical Review Letters. The results were embargoed until the seminar announcing the results on March 2, but a few days before, newspaper reporters had picked up the scent and reported on the impending announcement.

In the discovery publications [1, 2], CDF and D0 presented quite complementary analyses. CDF relied heavily on its b -tagging capability, and claimed a one in a million probability for the expected backgrounds to produce the observed yield of 6 dilepton events, 21 events with a b quark jet tagged by the vertex detector

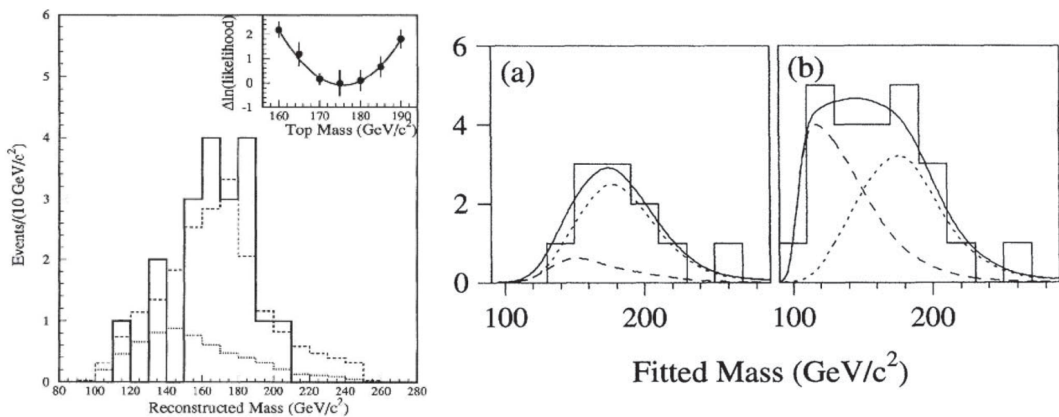


Figure 2: The reconstructed mass distribution of single lepton candidate events showing the data (solid histogram), the expected background and expected $t\bar{t}$ signal for the CDF (left) and D0 (right) measurements. The CDF panel inset shows the log-likelihood distribution as a function of assumed mass and the fit for the best mass value. The two elements of the D0 panel show the result for (a) the standard analysis and (b) for an analysis with loosened selection criteria.

(with 27 jets tagged) and 22 ℓ +jets events tagged by a muon within the jet (with 23 jets tagged), with an estimated background component of 1.3 dilepton events and 6.7 and 15.4 tagged jets for the two categories of single lepton events. D0 used stricter selection cuts based on the topological variables H_T , defined as the sum of the scalar E_T of the objects in the event, and the aplanarity, which measured the tendency for the momenta of the objects to lie in a plane, to suppress backgrounds. D0 found 3 dilepton events, 8 ℓ +jets events with the topological cuts and 6 events with a b jet tagged with a soft muon, with estimated backgrounds of 0.65, 1.9 and 1.2 events respectively for the three categories, with an estimated probability for background to fluctuate to the observed yields of two in a million. For the ℓ +jets events a measure of the top mass could be reconstructed from the four-momenta of the observed objects and a fit for the neutrino momentum using the W mass as a constraint. This fitted mass was then compared with a family of Monte Carlo templates with varied input masses to obtain the most likely top quark mass. Figure 2 shows the fitted mass distributions from the discovery papers. CDF obtained a mass of $m_t = 176 \pm 13$ GeV and D0 found $m_t = 199 \pm 30$ GeV. Using the observed yields and accounting for experimental efficiencies and acceptances, the cross section for $t\bar{t}$ pair production could be obtained. CDF found $\sigma(t\bar{t}) = 6.8_{-2.4}^{+3.6}$ pb and D0 obtained $\sigma(t\bar{t}) = 6.4 \pm 2.2$ pb. The results were consistent with each other, and with the modern measurements of the mass and cross section. D0 also presented the two-dimensional plot of the mass of two jets (from hadronic W decay) versus the three jet mass (the hadronic top decay) that supported the hypothesis for the

decay $t \rightarrow Wb$. Both collaborations saw an excess which was a little less than a 5σ deviation from a background-only hypothesis, but the joint result had more than 5σ significance and originated the modern standard of requiring 5σ for a discovery.

The strikingly large mass of the observed top quark stimulated the subsequent program of measurements described in the succeeding sections.

4 Top-antitop pair production

Up until 2009, the top quark could only be produced at the Tevatron. The 2001 – 2011 run acquired about 10 fb^{-1} of data using $p\bar{p}$ collisions at 1.96 TeV, or about 200 times that used for the 1995 discovery. In 2009, the Large Hadron Collider (LHC) came into operation using pp collisions, first at 7 TeV, increasing to 8 TeV in 2012 and then to 13 TeV in 2015. The general purpose ATLAS and CMS experiments have accumulated large samples of top quark events, augmented by data from the LHCb experiment in some kinematic regions.

The production of $t\bar{t}$ pairs proceeds through annihilation of a quark and an antiquark or through interaction of gluons in the colliding beam particles. At the Tevatron $p\bar{p}$ collider, the $q\bar{q}$ processes account for about 85% of the cross section whereas at the LHC pp , the gg process is dominant ($> 80\%$). Recently the full next-to-next-to-leading-order (NNLO) QCD calculations of the inclusive cross sections have been provided [38] with estimated uncertainties of 2.2% (Tevatron) or 3% (LHC) due to higher order contributions. Some differential cross sections at NNLO have also been calculated [39]. Precise measurements of inclusive and differential cross sections can thus give sensitive tests of the SM. Since the top quark decays prior to hadronization, information on the spin correlations and polarizations can also be obtained.

The Tevatron measurements of the inclusive $t\bar{t}$ cross section as of 2013 are summarized in Fig. 3(a). The combination of CDF and D0 results [40] yields $\sigma_{t\bar{t}} = 7.60 \pm 0.41 \text{ pb}$, in good agreement with the NNLO theoretical prediction [38] of 7.16 pb. Recent D0 updates of the ℓ +jets and dilepton channel cross sections using the full 9.7 fb^{-1} of data are combined to give $\sigma_{t\bar{t}} = 7.73 \pm 0.56 \text{ pb}$ [41]. The individual ATLAS and CMS inclusive cross measurements at $\sqrt{s} = 8 \text{ TeV}$ and their combination [42], $\sigma_{t\bar{t}} = 241.5 \pm 8.5 \text{ pb}$, shown in Fig. 3(b) are also in good agreement with the NNLO prediction [38] of 245.8 pb. Cross sections for the forward production of top quarks at 7 and 8 TeV consistent with SM predictions have recently been reported by the LHCb collaboration [43].

Measurements of differential cross sections offer a more sensitive way to seek new phenomena in the top quark sector. Many models postulate a special role for the top quark in coupling to new non-SM physics which could be revealed through resonances observed in the $t\bar{t}$ mass distribution, or departures from SM predictions

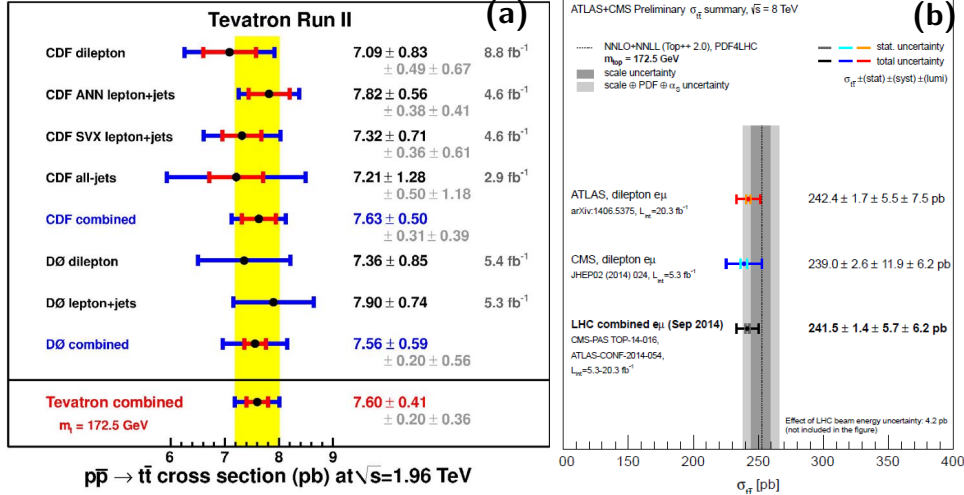


Figure 3: The $t\bar{t}$ inclusive cross section measurements at (a) the Tevatron and their combination; (b) the LHC and their combination.

in transverse momentum (p_T) or rapidity (y) distributions. Such distributions have been measured at the Tevatron [44] and more recently at the LHC [45] where the higher collision energy allows a much larger region of $m_{t\bar{t}}$ to be explored. To date, as shown in Fig. 4, no non-SM behavior has been seen for $m_{t\bar{t}} < 2.5 \text{ TeV}$.

Possible new physics coupling to the top quark can be sought through the production of heavy objects in association with a $t\bar{t}$ pair, particularly at the LHC where the available phase space is larger than at the Tevatron. New physics models such as supersymmetry predict such associated production final states, for example through the production of sbottom quark pairs with a decay chain $\tilde{b} \rightarrow t\tilde{\chi}_1^-$ and $\tilde{\chi}_1^- \rightarrow W^- \tilde{\chi}_1^0$ (and charge conjugate). Other models may enhance the SM cross sections for $t\bar{t} + X$ final states through new couplings (e.g. dimension six operators [46]). ATLAS and CMS have obtained evidence for the production of $t\bar{t}$ pairs with associated b or c quarks [47], W or Z bosons [48, 49, 50, 51], and $b\bar{b}$ [52], and have set limits on $t\bar{t}t\bar{t}$ production [53, 54, 55], all in good agreement with the SM prediction as shown in Fig. 5.

At leading order (LO), the annihilation of valence quarks and anti-quarks at the Tevatron is not expected to give a preference for t or \bar{t} to emerge in the proton hemisphere relative to the antiproton hemisphere. At next-to-leading-order (NLO), interferences between the LO Born and loop diagrams or initial and final state gluon radiation diagrams result in an expected small positive forward-backward asymmetry, $A_{FB}^{t\bar{t}} = (N(\Delta y > 0) - N(\Delta y < 0)) / (N(\Delta y > 0) + N(\Delta y < 0))$, where $\Delta y = y_t - y_{\bar{t}}$. The 2011 CDF measurement in the ℓ +jets channel with

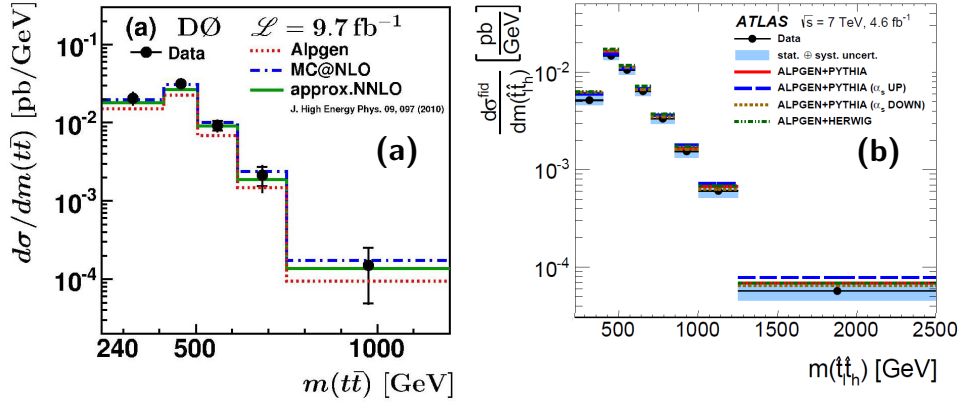


Figure 4: The differential cross section as a function of $m_{t\bar{t}}$ for (a) D0; (b) ATLAS.

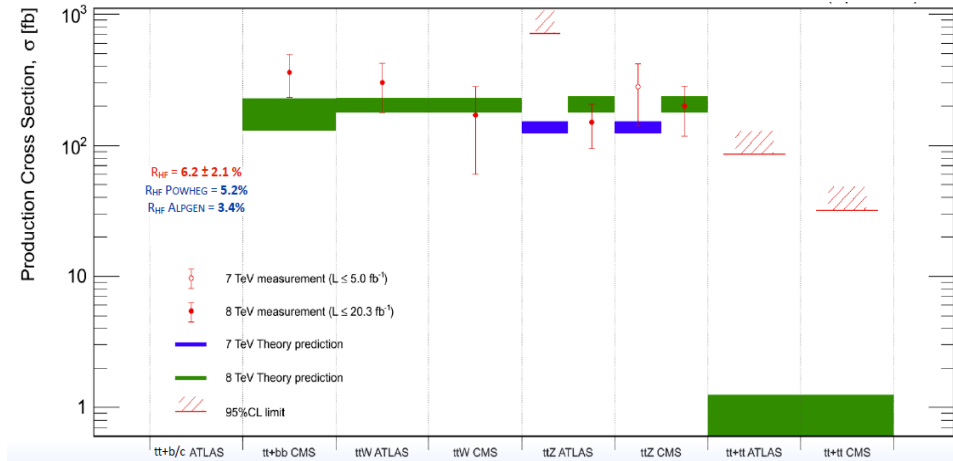


Figure 5: ATLAS and CMS measurements and limits for $t\bar{t}$ production in association with vector bosons and heavy quark pairs.

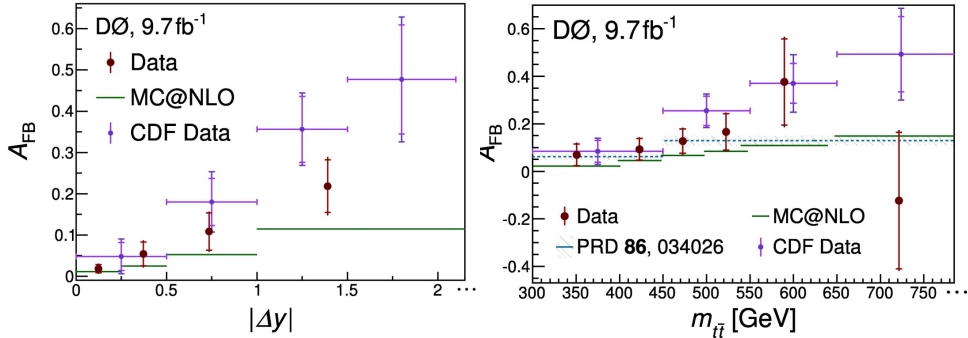


Figure 6: The D0 and CDF measurements of $A_{FB}^{t\bar{t}}$ as a function of Δy and $m_{t\bar{t}}$, compared with the NNLO QCD prediction with NLO electroweak corrections of Ref. [39].

5.3 fb^{-1} of data [56] in which the top quarks were unfolded to the parton level gave $A_{FB}^{t\bar{t}} = 0.158 \pm 0.074$, somewhat in tension with the then-existing NLO QCD prediction of about 0.06. The measured asymmetry grew both with Δy and $m_{t\bar{t}}$; for $m_{t\bar{t}} > 450 \text{ GeV}$, the discrepancy with NLO QCD reached 3.4σ . The 2011 D0 lepton+ jets measurement [57] found $A_{FB}^{t\bar{t}} = 0.092 \pm 0.037$, statistically compatible with both the CDF result and the NLO QCD prediction. These early measurements stimulated much theoretical activity [58] to find potential sources of new physics that could enhance the SM prediction, such as axigluon or Z' production.

By 2014, both the theoretical and experimental situations were clarified. A full NNLO calculation (thus next-to-leading order in the asymmetry) found $A_{FB}^{t\bar{t}} = 0.095 \pm 0.007$ [39]. Both CDF and D0 published results for the ℓ +jets channel with the full Tevatron data sample [59, 60], with inclusive asymmetry results $A_{FB}^{t\bar{t}} = 0.164 \pm 0.047$ and $A_{FB}^{t\bar{t}} = 0.106 \pm 0.030$ respectively. Figure 6 shows the results as a function of Δy and $m_{t\bar{t}}$ for both experiments and the NNLO predictions.

The reconstructed $t\bar{t}$ asymmetry in the dilepton channel has also been measured by D0 [61] to be $A_{FB}^{t\bar{t}} = 0.175 \pm 0.063$. A related lepton asymmetry $A_{FB}^{\ell} = (N(q_{\ell}\eta_{\ell}) > 0) - N(q_{\ell}\eta_{\ell}) < 0) / (N(q_{\ell}\eta_{\ell}) > 0) + N(q_{\ell}\eta_{\ell}) < 0)$, where q_{ℓ} is the sign of the lepton and η_{ℓ} is the pseudorapidity of the lepton, has been measured in the combined ℓ +jets and dilepton channels with results for CDF [62] and D0 [63] of $A_{FB}^{\ell} = 0.090_{-0.026}^{+0.028}$ and $A_{FB}^{\ell} = 0.047 \pm 0.027$ respectively, to be compared with the NLO prediction of 0.038 ± 0.003 [64]. The asymmetry in the pseudorapidity difference between the two lepton rapidities can be measured in the dilepton channel only and is consistent with NLO QCD in both experiments [65, 62].

Overall, the forward-backward asymmetries at the Tevatron have settled down to reasonable agreement with the most accurate predictions of QCD, with CDF

results typically exceeding the prediction by roughly 1.5σ and the D0 results in agreement with QCD within 1σ .

At the LHC, the pp initial state does not permit the definition of a forward or backward direction, so a central-forward asymmetry is defined instead: $A_C = (N(\Delta|y|) > 0) - N(\Delta|y| < 0))/(N(\Delta|y|) > 0) + N(\Delta|y| < 0))$, where $\Delta|y| = |y_t| - |y_{\bar{t}}|$. The NLO prediction for A_C is about 1% making this measurement difficult. Current preliminary measurements by ATLAS [66, 67] and CMS [68, 69, 70] are all consistent with $A_C = 0$ with uncertainties of 1 – 2%.

Since the top quark weak interaction decay is much shorter than the time required for hadronization by the strong interaction, the spin orientations of top quarks in production can be sensed through angular distributions of the decay products. Although in the SM, the polarizations of t or \bar{t} are expected to be close to zero, the correlation between the spin orientations is expected to be large. For the gg process that is dominant at the LHC, the gluons have mainly the same helicities at low $m_{t\bar{t}}$ and mainly opposite helicities at high $m_{t\bar{t}}$. At the Tevatron, production is mainly from an opposite helicity q and \bar{q} initial state, and thus the two colliders provide complementary information. The polar angle distributions of final state fermions in the $t\bar{t}$ rest frame can be written as

$$\frac{1}{\sigma} \frac{d\sigma}{d \cos \theta_1 \cos \theta_2} = \frac{1}{4} (1 + \alpha_1 \mathcal{P}_1 \cos \theta_1 + \alpha_2 \mathcal{P}_2 \cos \theta_2 + \alpha_1 \alpha_2 A \cos \theta_1 \cos \theta_2) \quad , \quad (1)$$

where θ_i is the decay fermion polar angle, \mathcal{P}_i is the polarization, α_i is the spin-analyzing power for particle i , and A is the spin correlation in the $t\bar{t}$ strong production process. The parameters α are near 1 for a charged lepton or down-type quarks, and 0.31 for up-type quarks. The spin quantization axes are chosen in the plane of scattering and can be taken to be the beam direction, the outgoing t -quark direction (helicity basis), or an intermediate axis chosen to obtain the maximum expected spin correlation. In the case of the production by the gg process, the distribution as a function of the azimuthal angle difference between decay leptons in dilepton events also carries information on the spin correlation.

D0's measurement of the spin correlation in the beam basis is $A = 0.85 \pm 0.29$ using both the lepton + jet and dilepton channels [71]. It is in good agreement with the SM prediction $A = 0.78^{+0.03}_{-0.04}$ [72] and 3.1σ away from the no-correlation hypothesis. CDF's measurement [73] in the helicity basis of $A = 0.60 \pm 0.22$ is also in good agreement with QCD. The first observations of a non-zero spin correlation were made by ATLAS [74] and CMS [75] using the azimuthal angle between the two leptons in the dilepton sample in dominantly gg interactions, for both the helicity basis and the intermediate basis. Subsequent addition of the lepton+jet channel allowed ATLAS [76] to measure several correlation observables in different bases which are sensitive to different types of new physics in $t\bar{t}$ production.

The top quark parity violating polarization in the plane of scattering is very

close to zero in the SM, so measurable non-zero polarization would signal new physics. The actual value of polarization depends upon the choice of basis for spin quantization; common choices are the helicity basis (the t quark momentum direction) or the beam basis (the incoming proton direction), both in the $t\bar{t}$ rest frame. A D0 determination of the polarization in the beam basis, $\mathcal{P} = 11.3 \pm 9.3\%$, was made in conjunction with the forward-backward asymmetry measurement in the dilepton channel [61]. Polarization measurements were recently performed by D0 in the $\ell + \text{jets}$ channel in the beam (helicity) basis with the, results $\mathcal{P} = 7.0 \pm 5.5\% (-10.2 \pm 6.0\%)$, as well as the parity conserving polarization normal to the scattering plane of $\mathcal{P} = 4.0 \pm 3.4\%$ [77]. Both ATLAS and CMS have measured polarizations at 7 TeV in the helicity basis. ATLAS determines CP even and CP odd polarizations of -0.035 ± 0.040 and 0.020 ± 0.022 [78]. CMS finds the CP even polarization to be 0.005 ± 0.021 [75].

Recently, the parity-violating polarization of single top quarks produced by the weak interaction has been measured [79] to be $\mathcal{P} = 0.82 \pm 0.34$, in good agreement with the NLO SM prediction of about 0.88.

5 Single top production

Top quarks are mainly produced as $t\bar{t}$ pairs at hadron colliders via the strong interaction. It was in this process that the top quark was discovered at the Tevatron and in which the majority of the top quark studies were performed. But as first proposed in [80], top quarks could also be produced singly in high energy collisions via the two electroweak processes shown in Fig. 7. A third process in which a top quark is produced in association with W boson has negligible cross section at the Tevatron but becomes important at the LHC as discussed below. The dominant t -channel process proceeds through the exchange of a space-like virtual W boson between a light (u, d, c, s) quark and a b quark. The subdominant process involves the exchange of a time-like virtual W boson in the s -channel producing a top quark and a b quark.

The production cross sections at the Tevatron are 1.12 pb (s -channel) and 2.34 pb (t -channel) [81]. Somewhat surprisingly, the total electroweak single top quark cross section is about half that for strong interaction $t\bar{t}$ pair production value of 7.16 pb [38]. The main reason is that the effective mass of the final state products in single top production is about half that for pair production, so that the much more abundant lower momentum quarks and gluons in the interacting proton and antiproton are required. However the smaller number of jets and leptons in single top production compared with $t\bar{t}$ production makes single top quark detection difficult due to the more copious backgrounds. Thus about 50 times more luminosity and 14 more years were required to discover electroweak

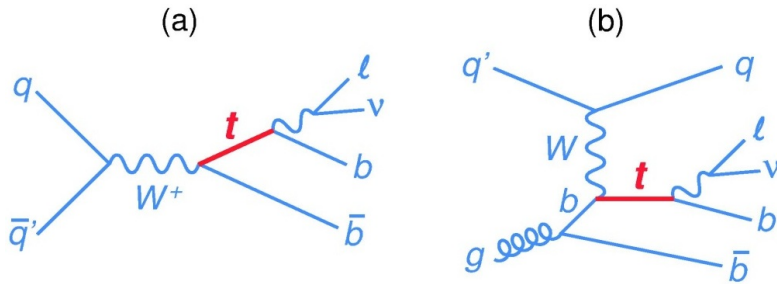


Figure 7: Feynman diagrams of the single top quark production via (a) s -channel process and (b) t -channel process.

single top quark production after the top quark discovery in pair production via the strong force.

The observation of single top quark production was reported by the CDF and D0 collaborations in 2009 using about 3 fb^{-1} of Tevatron data [82, 83]. The large W +jets background, with its higher cross section but similar final event topology (Fig. 7), posed the major challenge. After an initial “cut based” events selection on the kinematic parameters of the events, the signal fraction in the analysis sample was only $\approx 5\%$, well below the uncertainty on the background prediction. The only option for firmly establishing the existence of the single top quark events was the use of multivariate analysis methods [84, 85] which combine tens of event parameters into a single discriminant that provides good separation of signal and background. This discriminant uses not just the difference in signal and background distributions in each parameter but also the correlations among them. The multivariate classifiers were trained on large Monte Carlo samples of signal and background events. Discriminant distributions are shown in Fig. 8 for the CDF and D0 discovery analyses in which single top quark events concentrate at the large values of the discriminant. The discovery of single top quark production not only firmly established that electroweak single top production conforms to the SM prediction, but also verified for the first time that the power of the multivariate analyses could be used for particle physics discoveries. Many subsequent discoveries in particle physics, including that of the Higgs boson, relied heavily on the multivariate methods developed at the Tevatron for the single top quark production observation. These searches also spawned the development of new theoretical tools such as the single top quark event generators [86].

With 10 fb^{-1} per Tevatron experiment accumulated by the end of the Tevatron run together with improvements in the analysis methods, precise studies of the single top quark production became possible, including the independent observation of the single top quark t -channel and s -channel processes and measurement of their cross sections. The combination of CDF and D0 results was required for

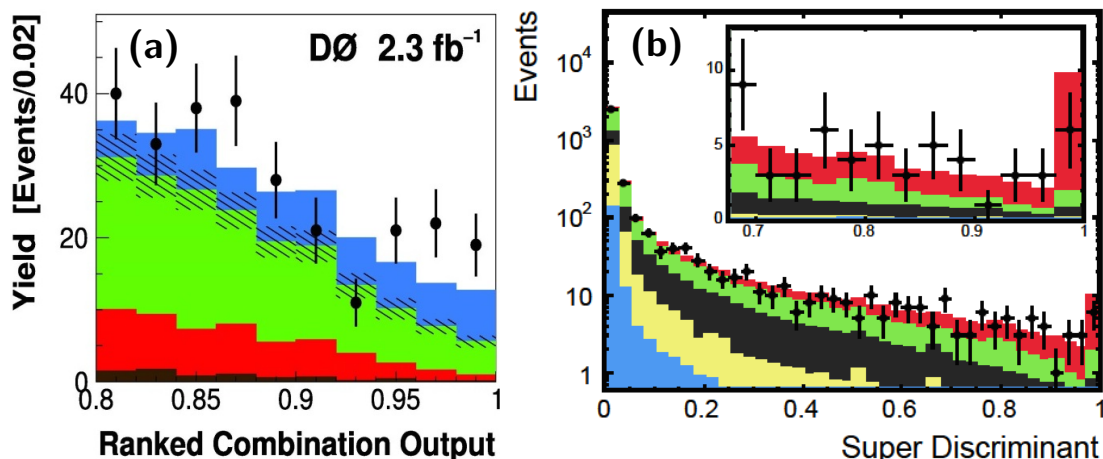


Figure 8: Observation of the single top quark production at the Tevatron. The D0 discriminant distribution is represented in (a), where the single top quark signal is shown in blue and shaded areas indicate the background uncertainty. The CDF discriminant distribution is presented in (b), indicating an excess of events at the large discriminant values in comparison with background predictions (non-red colors). Red indicates the single top quark contribution.

the 6.3σ observation of s -channel process [87]. Figure 9 summarizes single top quark production data at the Tevatron using full data set. The s - and t -channel cross sections are in agreement with the SM predictions.

The single top quark production cross section in the SM is approximately proportional to the square of the CKM matrix [11, 12] element V_{tb} . By extracting V_{tb} from the measured single top quark cross sections and including uncertainties on the predictions, this parameter is measured directly without assumptions on the number of quark generations or on the unitarity of the CKM matrix. The Tevatron measurement, $V_{tb} = 1.02^{+0.06}_{-0.05}$, shown in Fig. 10 is in agreement with the V_{tb} value obtained with the assumptions of CKM matrix unitarity and three quark generations [88].

The single top t -channel cross section at the LHC of 90 pb at $\sqrt{s} = 8$ TeV [89] is substantially larger than at the Tevatron and thus provides large samples of the single top quark events. An interesting feature of the LHC is that about twice as many top as anti-top quarks are produced due to the proton proton initial state (for the Tevatron these numbers are the same). All measured single top quark cross sections and ratios of the top to anti-top cross sections at 7 TeV and 8 TeV LHC energies are in agreement with the SM predictions. The s -channel cross section at the LHC (3.2 pb at $\sqrt{s} = 7$ TeV [90]) has a relatively small increase over the Tevatron as this process requires quark-anti-quark annihilation (Fig. 7)

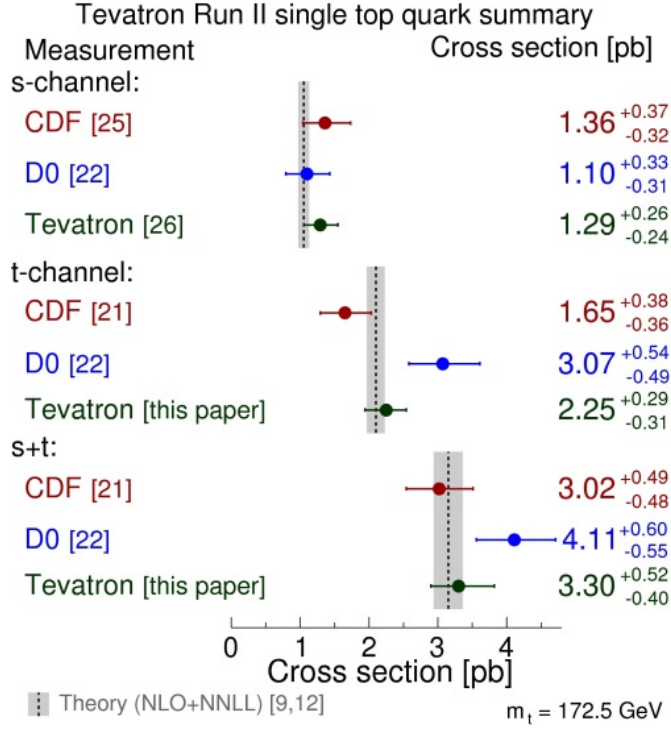


Figure 9: Tevatron single top quark cross sections summary, taken from [88]. Reference numbers in the figure are those from that paper.

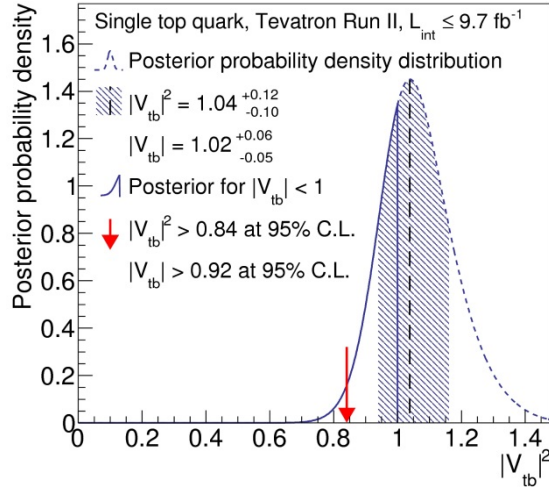


Figure 10: Posterior probability distribution as a function of $|V_{tb}|^2$ for the combination of CDF and D0 results.

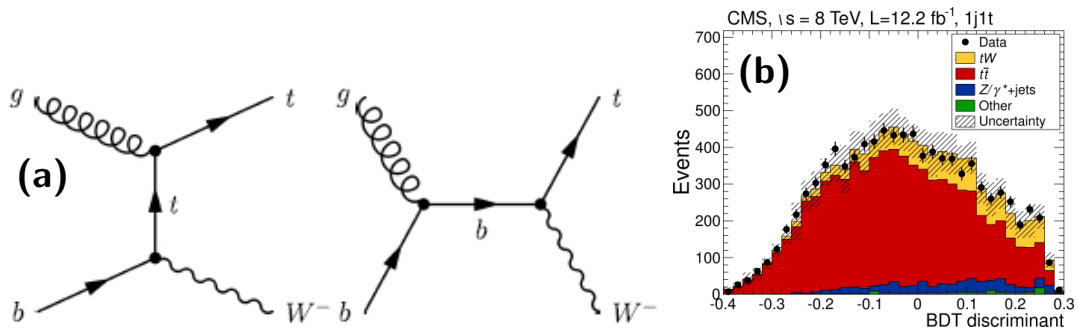


Figure 11: Leading order Feynman diagrams of associated W and top quark production (a) and CMS observation of the associated tW production (b).

which only sea quarks at the LHC provide. As backgrounds for the s -channel process increase rapidly with energy, this channel has not yet been observed at the LHC. In addition to the s -channel and t -channel production single top quarks can be produced in association with a W boson, called tW -channel, as shown in the Fig. 11. The cross section for this process at 8 TeV is 22 pb [91]. While this cross section is substantial, top quark pair production creates substantial background. The CMS experiment, using 12 fb^{-1} of $\sqrt{s} = 8 \text{ TeV}$ collisions and multivariate analysis methods, was able to observe tW associated production with 6.1σ significance, completing the observation of all leading order processes of single top quark production [92].

6 Top quark mass

6.1 Direct measurements

Measurements of the top quark mass, m_t , using kinematic properties of the decay products of the top quark, i.e., using *direct* approaches, have been performed by the ATLAS, CDF, CMS, and DØ Collaborations using a variety of experimental techniques. These experimental techniques can be grouped into three categories:

- The **template method** uses probability densities (PD), often referred to as “templates”, of the distributions of kinematic observables related to the top quark mass, such as the invariant mass of the trijet system from the $t \rightarrow q\bar{q}'b$ decay. The templates are constructed using simulated MC events, where the signal templates are parametrised as a function of m_t and possibly other parameters such as the jet energy correction factors. The sensitivity to m_t is established by comparing the distribution(s) of selected observable(s) in data to the templates as a function of m_t and possibly other parameters,

for example, with a maximum likelihood fit.

- The **matrix element method** calculates *ab initio* the PD P_{evt} , as a function of m_t and possibly other parameters, for a given event to be observed under the hypotheses of top quark production, P_{sig} , or of a background process, P_{bgd} , where $P_{\text{evt}} = fP_{\text{sig}} + (1 - f)P_{\text{bgd}}$ and f is the fraction of signal events in the sample, determined from data. The PDs P_{sig} and P_{bgd} are expressed through their respective matrix elements (MEs) \mathcal{M}_{sig} and \mathcal{M}_{bgd} , taking into account the experimental resolution of the jets and leptons measured in the detector. The MEs \mathcal{M} are sums over all contributors at a given order.. Typically, all possible jet-parton assignments are considered, and weighted by their consistency with the b -tagging information. The method establishes the sensitivity to m_t by calculating P_{evt} as a function of m_t , and maximizing the combined likelihood for all observed events.
- The **ideogram method** can be considered an approximation of the ME method, since it also calculates a *per-event* PD under the $t\bar{t}$ and background hypotheses. By contrast to the ME method, P_{sig} is calculated using a kinematic fit of the decay products of the top quark to its Breit-Wigner resonance within their respective experimental resolutions. All possible jet-parton assignments are summed, typically weighted by their consistency with the b -tagging information, and by the negative logarithm of the χ^2 of their kinematic fit. The combined likelihood of all observed events is then maximised to establish sensitivity to m_t .

The advantage of the template method is that it is intuitive and straightforward in the sense that no calibration of the analysis is needed since the templates are constructed directly from simulated MC events. This was the method used to estimate the top quark mass in the discovery papers [1, 2]. The advantage of the ME technique is that it provides the highest possible statistical sensitivity according to the Neyman-Pearson lemma [93] by analysing the full four-vectors of the measured final state objects under *fundamental* signal and background hypotheses. It also provides a more accurate estimation of systematic uncertainties, as it evaluates their impact following a concrete model described by $|\mathcal{M}_{\text{sig}}|^2$, $|\mathcal{M}_{\text{bgd}}|^2$, and the experimental resolutions. A disadvantage of the ME method is its high computational demand. The ideogram method has the advantage that it is considerably less computationally demanding than the ME method.

A summary of the most precise recent direct measurements of m_t from the ATLAS, CDF, CMS, and DØ Collaborations is given in Table 2, and an overview of the measured values is presented in Fig. 12. In the following, we review three representative measurements using the three experimental techniques above.

Collab.	Channel	Method	\sqrt{s} (TeV)	$\int \mathcal{L} dt$ (fb $^{-1}$)	$m_t \pm (\text{stat}) \pm (\text{syst})$ (GeV)	Uncert.	Ref.
ATLAS	$\ell\ell\&\ell+j$	template	7	4.7	$172.99 \pm 0.48 \pm 0.78$	0.53%	[94]
ATLAS	single t	template	8	20.3	$172.2 \pm 0.7 \pm 2.0$	1.2 %	[95]
ATLAS	all-jets	template	7	4.7	$175.1 \pm 1.4 \pm 1.2$	1.1 %	[96]
CDF	$\ell\ell$	template	1.96	9.1	$170.80 \pm 1.83 \pm 2.69$	1.90%	[97]
CDF	$\ell+jets$	template	1.96	8.7	$172.85 \pm 0.71 \pm 0.85$	0.64%	[98]
CDF	all-jets	template	1.96	9.3	$175.07 \pm 1.19 \pm 1.56$	1.12%	[99]
CDF	\cancel{E}_T+j	template	1.96	8.7	$173.93 \pm 1.64 \pm 0.87$	1.07%	[100]
CMS	$\ell\ell$	template	8	19.7	$172.3 \pm 0.3 \pm 1.3$	0.7 %	[101]
CMS	$\ell+jets$	ideogram	8	19.7	$172.04 \pm 0.19 \pm 0.75$	0.45%	[102]
CMS	all-jets	ideogram	8	18.2	$172.08 \pm 0.27 \pm 0.86$	0.52%	[103]
D0	$\ell\ell$	template	1.96	9.7	$173.32 \pm 1.36 \pm 0.85$	0.93%	[104]
D0	$\ell+jets$	ME	1.96	9.7	$174.98 \pm 0.41 \pm 0.63$	0.43%	[105]

Table 2: Overview of recent direct measurements of m_t . Only the most precise measurement in a given channel is shown for each experiment. The channel labelled as “ $\ell\ell\&\ell+j$ ” combines the results in the $\ell\ell$ and $\ell+jets$ channels. The label “single t ” represents topologies enriched with production of single top quarks. The channel labelled as “ \cancel{E}_T+j ” corresponds to $\ell+jets$ events where the charged lepton is missed.

ATLAS recently performed a measurement of m_t in the $\ell\ell$ channel in pp collision data at $\sqrt{s} = 7$ TeV using 4.7 fb^{-1} of integrated luminosity [94]. This analysis applies a *template method* to the $m_{\ell b}$ observable, which is defined as the average invariant mass of the charged lepton and the b quark from the $t \rightarrow W(\ell^+\nu)b$ and $\bar{t} \rightarrow W(\ell^-\bar{\nu})\bar{b}$ decays. This observable was shown to provide less dependence on systematic uncertainties than other observables [106]. The result is $m_t = 173.79 \pm 0.54$ (stat) ± 1.30 (syst) GeV.

A measurement of m_t in the $\ell+jets$ channel in pp collisions at $\sqrt{s} = 8$ TeV was carried out by CMS using 19.7 fb^{-1} of integrated luminosity [102]. The analysis was performed with a *ideogram method*. Like most measurements of m_t in the $\ell+jets$ and all-jets channels, this analysis performs an *in situ* calibration of the overall jet energy scale correction factor, k_{JES} , by constraining the invariant mass of the dijet system associated with the $W \rightarrow q'\bar{q}$ decay to $m_W = 80.4$ GeV [107]. The result was $m_t = 172.04 \pm 0.19$ (stat) ± 0.75 (syst) GeV.

The current most precise single measurement of m_t was performed by D0 in the $\ell+jets$ channel in $p\bar{p}$ collisions at $\sqrt{s} = 1.96$ TeV using 9.7 fb^{-1} of integrated luminosity [105, 108]. This analysis applies an improved implementation of the *ME method* [109], which requires only 1% of the computation time needed previously [110]. This measurement substantially reduces the overall uncertainty relative to the previous measurement [110] through an improved estimation of

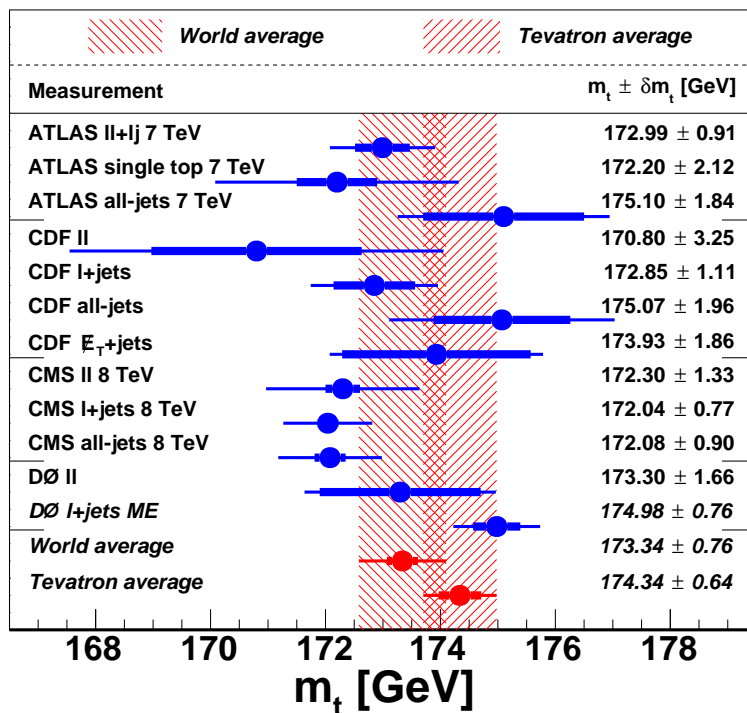


Figure 12: Overview of recent direct measurements of m_t . Only the most precise measurement in a given channel is shown for each experiment. The statistical uncertainty is indicated by the thick inner error bars, while the total uncertainty is shown by the thin outer error bars. The uncertainty given as δm_t represents the total uncertainty. For references to the measurements cf. Table 2.

the dominant uncertainties from the modelling of $t\bar{t}$ events and of the detector response. As shown in Fig. 13(a) a simultaneous fit to m_t and the jet energy scale factor k_{JES} was made using the W boson mass constraint. The result was $m_t = 174.98 \pm 0.41$ (stat) ± 0.63 (syst) GeV.

The first world combination of m_t measurements was performed in 2014 using BLUE [111, 112] and taking into account the correlations between the colliders, experiments, and analysis channels for all sources of systematic uncertainty considered [10]. The combined value is $m_t = 173.34 \pm 0.27$ (stat) ± 0.71 (syst) GeV, which corresponds to a relative uncertainty of 0.44%. Many of the recent measurements shown in Table 2 were not included in Ref. [10], and substantial improvement is expected for the next world combination.

Currently, the world's most precise direct experimental determination of m_t comes from the recent Tevatron combination, which includes all results from the CDF and DØ Collaborations given in Table 2 except Ref. [104], and in addition includes the m_t results from Run I of the Tevatron at $\sqrt{s} = 1.8$ TeV [113]. The

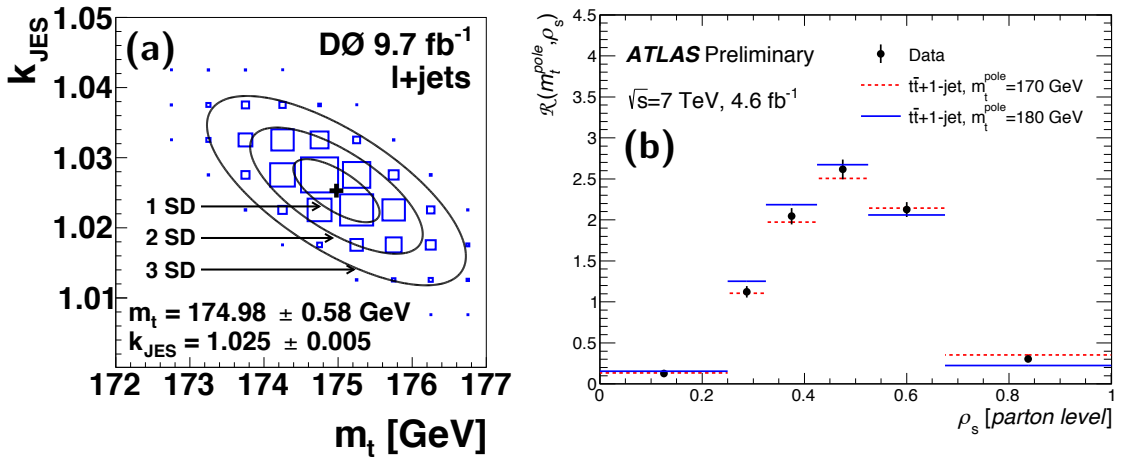


Figure 13: Two-dimensional likelihood in (m_t, k_{JES}) for the world’s most precise direct measurement of m_t [105] is shown in (a). Fitted contours of equal probability are overlaid as solid lines. The maximum is marked with a cross. The measured values with purely statistical uncertainties are given, where the statistical uncertainty from k_{JES} is propagated to the uncertainty on m_t . The distribution $1/\sigma_{t\bar{t}+1\text{jet}} \cdot d\sigma_{t\bar{t}+1\text{jet}}/d\rho_s$, denoted as \mathcal{R} , is presented in (b) at parton level for the world’s most precise single measurement of m_t^{pole} [127]. The dashed and continuous lines correspond to the SM expectation for $m_t^{\text{pole}} = 170$ and 180 GeV, respectively. The uncertainties shown in (a) and (b) are purely statistical.

combination is performed with BLUE using a similar categorisation of systematic uncertainties to that of the world combination. The combined Tevatron result of $m_t = 174.34 \pm 0.37$ (stat) ± 0.52 (syst) GeV corresponds to a relative precision of 0.37%.

6.2 Indirect measurements

For a free particle with four-momentum p , the physical mass is usually taken as the pole of its propagator $1/(p^2 - (m^{\text{pole}})^2)$. Because of confinement, quarks cannot exist as free particles, and this definition becomes uncertain at the level of $\Lambda_{\text{QCD}} \approx 0.2$ GeV [114, 115, 116]. An alternative mass definition, $m_t^{\overline{\text{MS}}}$, is given in the modified minimal subtraction renormalisation scheme [117]. The $\overline{\text{MS}}$ mass is also often referred to as the “running mass” $m_t(\mu_R)$, which alludes to the main idea to absorb the logarithmic corrections from soft QCD effects into the explicit dependence on the renormalization scale μ_R , resulting in a better numerical behaviour of perturbative predictions. Other mass definitions have been also suggested [118, 119].

All direct measurements of m_t rely on simulated MC events, and therefore on the mass parameter used in MC event generators, m_t^{MC} . This introduces a dependence of the directly measured m_t on the theory model used to describe the showering of final state quarks or gluons, and the subsequent hadronization process. As a result, m_t^{MC} is subject to a systematic uncertainty of the order of Λ_{QCD} [120], which is explicitly accounted for in the measurements. The numerical values of m_t in the different definition schemes can differ significantly. For example, at NNLO, the difference between m_t^{pole} and $m_t^{\overline{\text{MS}}}$ is ≈ 10 GeV. The definition m_t^{MC} in state-of-the-art MC generators does not absorb any corrections from parton showering or hadronization, and therefore corresponds approximately to m_t^{pole} , with an ambiguity of up to 1 GeV [119, 120].

The first *indirect* measurements of m_t that avoided the ambiguity between m_t^{MC} and m_t^{pole} were performed by CDF [121] and D0 [122] in 2008. These measurements extracted $m_t^{\text{pole}} = 178_{-10}^{+11}$ GeV and $m_t^{\text{pole}} = 170 \pm 7$ GeV from the top quark pair cross section, $\sigma_{t\bar{t}}$, measured in the $\ell\bar{\ell}$ and ℓ +jets channels using integrated luminosities of 1.2 and 0.9 fb $^{-1}$, by relating the experimental result to the NLO [123] and approximate NNLO predictions [38], respectively.

The world's most precise single measurement of m_t^{pole} from $\sigma_{t\bar{t}}$, with an uncertainty of 2.6 GeV, was performed by ATLAS in the $e\mu$ channel using pp collision data at $\sqrt{s} = 7$ and 8 TeV [124]. This measurement profits from a small experimental uncertainty of $\approx 4\%$ and the advent of the full NNLO calculation of $\sigma_{t\bar{t}}(m_t^{\text{pole}})$ [38], including NNLL corrections, which has a substantially reduced uncertainty relative to the approximate NNLO results. A similar measurement was performed by CMS, which achieves an uncertainty of 2.9 GeV [125].

Recently, ATLAS applied a novel approach [126] to measure m_t^{pole} from the production cross section of $t\bar{t}$ events in association with a hard jet $\sigma_{t\bar{t}+1\text{jet}}$ [127], as a function of the inverse of the invariant mass of the $t\bar{t}+1$ jet system $\rho_s \propto 1/\sqrt{s_{t\bar{t}+1\text{jet}}}$, and achieved a precision on m_t^{pole} of 2.2 GeV. The normalised unfolded distribution $1/\sigma_{t\bar{t}+1\text{jet}} \cdot d\sigma_{t\bar{t}+1\text{jet}}/d\rho_s$ is compared to NLO calculations [126] as a function of m_t^{pole} in Fig. 13(b). Recent measurements of m_t^{pole} are summarised in Table 3.

7 Top quark properties

Unlike the top quark mass, the SM predicts all other properties of top quarks and their decays with high precision. Since the top quark lifetime is much shorter than the time required for hadronization, top quark properties can be measured directly and usually with much less uncertainty than those for other quarks where these characteristics are derived from their bound states. Differences between measured properties and the precisely known SM predictions offer sensitive tests for new physics beyond the SM.

Collab.	Channel	From	\sqrt{s} (TeV)	$\int \mathcal{L} dt$ (fb ⁻¹)	m_t (GeV)	Relative uncert.	Reference	
							Exp.	Theory
ATLAS	$e\mu$	$\sigma_{t\bar{t}}$	7	4.6	$171.4^{+2.6}_{-2.6}$	+1.5% -1.5%	[124]	[38]
ATLAS	$e\mu$	$\sigma_{t\bar{t}}$	8	20.3	$174.1^{+2.6}_{-2.6}$	+1.5% -1.5%	[124]	[38]
ATLAS	$l+\text{jets}$	$\sigma_{t\bar{t}+1\text{jet}}$	7	4.6	$173.7^{+2.3}_{-2.1}$	+1.3% -1.2%	[127]	[126]
CDF	ll	$\sigma_{t\bar{t}}$	1.96	1.2	$178.3^{+10.9}_{-9.9}$	+6.1% -5.5%	[121]	[123]
CMS	ll	$\sigma_{t\bar{t}}$	7	2.3	$176.7^{+3.0}_{-2.8}$	+1.7% -1.6%	[125]	[38]
DØ	$ll\&l+j$	$\sigma_{t\bar{t}}$	1.96	9.7	$169.4^{+3.6}_{-3.8}$	+2.1% -2.2%	[41]	[38]

Table 3: Overview of recent indirect measurements of m_t^{pole} . The channel labelled as “ $ll\&l+j$ ” combines the results in the ll and $l+\text{jets}$ channels. The total uncertainty quoted corresponds to the quadratic sum of the full experimental uncertainty and the entire theory uncertainty.

7.1 Top quark lifetime

The lifetime τ and the related resonance width $\Gamma = 1/\tau$ are primary characteristics of any particle. Due to its large mass, a small value of the top lifetime, τ_t , is expected. The SM predicts $\Gamma_t = 1.32$ GeV [128] with about 1% uncertainty, or $\tau_t = 4.99 \times 10^{-25}$ s. It is impossible to measure such a short lifetime directly by measuring the distance between birth and decay as done for example, for B -mesons; nevertheless the CDF Collaboration undertook such a measurement, finding $\tau_t < 2 \times 10^{-13}$ s [129].

An alternative approach used for strongly interacting decays is a direct measurement of the width. To use this method the experimental mass resolution of the experiment should be better than the expected width. Unfortunately all Tevatron and LHC experiments have mass resolutions worse than the SM Γ_t value. The most precise measurement of the top quark width was obtained by CDF [130] using 8.7 fb^{-1} of data. They obtain $1.10 < \Gamma_t < 4.05$ GeV, corresponding to $1.6 \times 10^{-25} < \tau_t < 6.0 \times 10^{-25}$ s at 68% confidence level (CL), in agreement with SM prediction.

The D0 Collaboration used an indirect method to obtain Γ_t [131] under the assumption that $\Gamma(t \rightarrow Wb)$ is proportional to the measured t -channel single top quark production cross-section with the proportionality factor $\Gamma(t \rightarrow Wb)/\sigma(t\text{-channel})$ as predicted by SM. The width is then obtained from $\Gamma_t = \Gamma(t \rightarrow Wb)/\mathcal{B}(t \rightarrow Wb)$, where $\mathcal{B}(t \rightarrow Wb)$ is the branching ratio for $t \rightarrow Wb$. Using the experimental values $\sigma(t\text{-channel}) = 2.90 \pm 0.59$ pb [132], $\mathcal{B}(t \rightarrow Wb) = 0.90 \pm 0.04$ [133] and the SM predictions $\Gamma(t \rightarrow Wb) = 1.33$ GeV [107], $\sigma(t\text{-channel}) = 2.14 \pm 0.18$ pb [81], they obtain $\Gamma_t = 2.00^{+0.47}_{-0.43}$ GeV and $\tau_t =$

Experiment	$m_t - m_{\bar{t}}$ (GeV)
D0 [140]	0.8 ± 1.8 (stat) ± 0.5 (syst)
CDF [141]	-1.95 ± 1.11 (stat) ± 0.59 (syst)
CMS [142]	-0.44 ± 0.46 (stat) ± 0.27 (syst)
ATLAS [143]	0.67 ± 0.61 (stat) ± 0.41 (syst)

Table 4: Mass differences of top and antitop quarks measured at the Tevatron and the LHC.

$3.29_{-0.63}^{+0.90} \times 10^{-25}$ s. This indirect method was also used by CMS [134] with parameters from Refs. [107, 134, 135, 136] to obtain $\Gamma_t = 1.36 \pm 0.02$ (stat) $_{-0.11}^{+0.14}$ (syst) GeV, in a good agreement with SM prediction.

7.2 t and \bar{t} mass difference

The CPT theorem, based on the general principles of local relativistic quantum field theory, predicts that antiparticle properties are the same as the corresponding particle properties after spatial and time coordinate inversions. In particular, particle and antiparticle masses must be the same. Although CPT symmetry is rigorously conserved in the SM, some SM extensions permit CPT invariance breaking [137, 138, 139]. A stringent limit on particle-antiparticle mass inequality was obtained for the $K^0 - \bar{K}^0$ system: $(m_{K^0} - m_{\bar{K}^0})/m_{K^0} < 0.6 \times 10^{-18}$ at 90% CL [107], but the SM extensions allow different quark flavors to have different CPT -violating couplings. The experimental results of top – antitop mass difference shown in Table 4 are in good agreement with invariance under the CPT transformation. The charge of the lepton from W boson decay in $t \rightarrow Wb$ is used to tag top versus antitop quarks.

7.3 Top quark electric charge

In the SM the top quark has an electric charge of $+2/3e$ and decays to W^+ and a charge $-1/3$ quark (dominantly b). But in an extension of SM [144, 145], an exotic quark with mass of about 170 GeV and charge $-4/3e$ occurs as a part of a fourth quark generation with decay to W^-b , while the SM top quark mass is expected to be heavier than 230 GeV. The first limit on a $-4/3e$ top quark was obtained by D0 in 2007 [146]; more recently D0 reported [147] the analysis of 286 fully reconstructed $t\bar{t}$ pairs in the ℓ +jets channel. The results shown in Fig. 14(a) rule out a $-4/3e$ exotic top quark at a significance greater than 5σ and set an upper limit on the exotic quark fraction of 0.46 at 95% CL.

The CDF Collaboration performed an analysis in the ℓ +jets channel [148]. The W boson charge Q_W was determined from the decay lepton charge. The associated

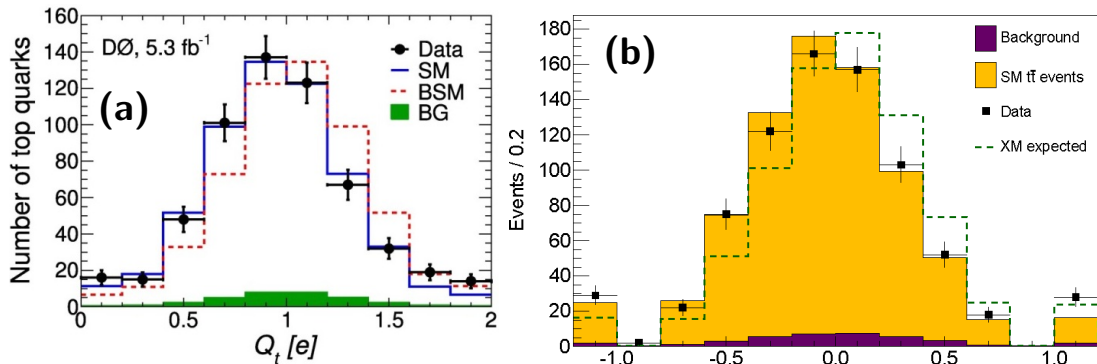


Figure 14: (a) Combined distribution in the charge Q_t for $t\bar{t}$ candidates in D0 data compared with expectations from the SM and the BSM from Ref. [147]. The background contribution (BG) is represented by the green-shaded histogram. (b) Distribution of the product of the W boson charge times the Q_{jet} value from CDF. Shaded histograms show signal and background predictions stacked for the total prediction. The dashed line shows expectation from an exotic model (XM) [144, 145]. SM-like candidates are on the negative side of the plot while XM-like candidates are on the positive side. The outermost bins correspond to the cases where $Q_{\text{jet}} = \pm 1$.

Channel	Q_t in units of electron charge
e +jets	0.63 ± 0.04 (stat) ± 0.11 (syst)
μ +jets	0.65 ± 0.03 (stat) ± 0.12 (syst)
ℓ +jets	0.64 ± 0.02 (stat) ± 0.08 (syst)

Table 5: The ATLAS results of the top quark charge measurements.

jet charge Q_{jet} was reconstructed with special jet charge algorithm. A negative value of the product $Q_W \cdot Q_{\text{jet}}$ corresponds to the SM $t\bar{t}$ decay while a positive product comes from the exotic $t\bar{t}$ decay. The results shown in Fig. 14(b) exclude an exotic top quark with $-4/3e$ charge and mass of about 170 GeV at the 99% CL

The most stringent limit on the existence of a $-4/3e$ quark with mass of about 170 GeV was given by ATLAS [149]. The results [149] are shown in Table 5. The results for the e and μ channels are in good agreement and coincide with SM prediction ($2/3e$) within the errors quoted. They exclude the XM model [144] with a significance of more than 8σ . This model also disagrees with the results on single top production as well [150, 151].

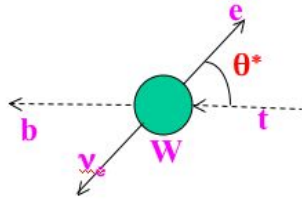


Figure 15: Definition of helicity angle θ^* .

Experiment	f	Results
D0+CDF [154]	f_0	0.722 ± 0.081 [± 0.062 (stat) ± 0.052 (syst)]
	f_+	-0.033 ± 0.046 [± 0.034 (stat) ± 0.031 (syst)]
CDF [155]	f_0	0.726 ± 0.066 (stat) ± 0.067 (syst)
	f_+	-0.045 ± 0.044 (stat) ± 0.058 (syst)
ATLAS [156]	f_0	0.67 ± 0.07
	f_-	0.32 ± 0.04
	f_+	0.01 ± 0.05
CMS [157]	f_0	0.720 ± 0.039 (stat) ± 0.037 (syst)
	f_-	0.298 ± 0.028 (stat) ± 0.032 (syst)
	f_+	-0.018 ± 0.019 (stat) ± 0.011 (syst)

Table 6: Results of the helicity fraction f measurements.

7.4 W boson polarization in top quark decays

The helicities of W bosons in top quark decays can be $+1$, -1 or 0 , corresponding to right-handed, left-handed or longitudinal polarizations, with corresponding fractions of events in the decay $t \rightarrow Wb$ of f_+ , f_- or f_0 respectively. These fractions can be measured using the event distribution in $\cos \theta^*$ [152] where θ^* is the angle between the charged lepton momentum and the negative of the top quark momentum in the W boson rest frame (see Fig. 15):

$$\frac{1}{\sigma} \frac{d\sigma}{d\cos \theta^*} = \frac{3}{4} (1 - \cos^2 \theta^*) f_0 + \frac{3}{8} (1 - \cos \theta^*)^2 f_- + \frac{3}{8} (1 + \cos \theta^*)^2 f_+ .$$

The SM predicts [153] $f_0 = 0.687 \pm 0.005$, $f_- = 0.311 \pm 0.005$, and $f_+ = 0.0017 \pm 0.0001$. Deviation from these values would indicate new physics beyond the SM.

Results are presented in Table 6 and Fig. 6. The experimental results are consistent and agree well with SM expectations for helicity fractions, and with the $V - A$ structure of the Wtb vertex.

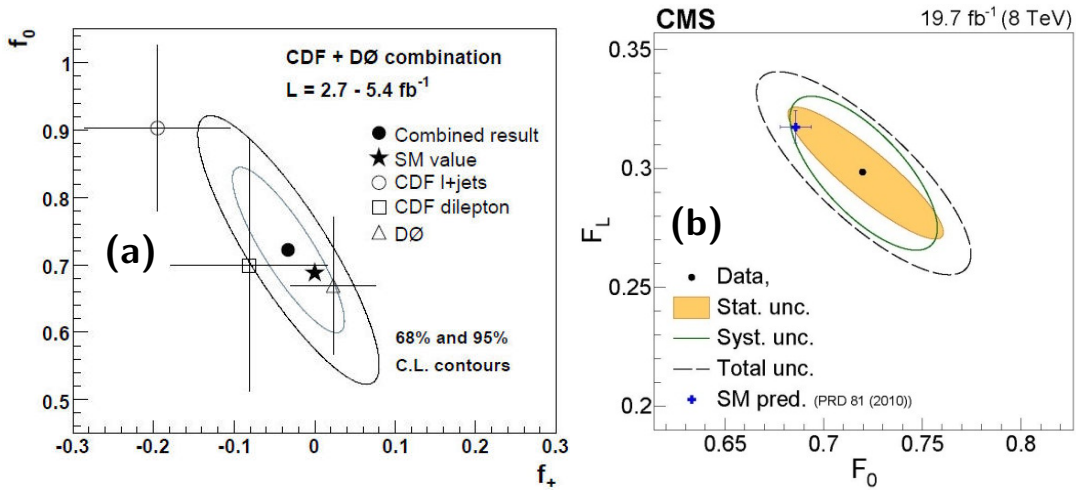


Figure 16: (a) Contours of constant χ^2 for the Tevatron combination of the 2D helicity measurements [154]. The ellipses indicate the 68% and 95% CL contours, the dot shows the best-fit value, and the star marks the expectation from the SM. Each of the input measurements uses a central value of $m_t = 172.5$ GeV. (b) Combined results from the CMS muon+jets and electron+jets events for the left-handed and longitudinal W boson helicity fractions [157], shown as 68% contours for statistical, systematic, and total uncertainties, compared to the SM predictions [153].

Experiment	R	$ V_{tb} $	lower limit at 95% CL,
D0 [133]	0.90 ± 0.04	0.95 ± 0.02	n/a
CDF [159]	0.87 ± 0.07	0.93 ± 0.04	> 0.85
CDF [160]	0.94 ± 0.09	0.97 ± 0.05	> 0.89
CMS [134]	1.014 ± 0.032	n/a	> 0.975 (> 0.955 $R \leq 1$)

Table 7: Results of the measurements of the ratio R and $|V_{tb}|$ in $t\bar{t}$ events.

7.5 V_{tb} element of Cabibbo-Kobayashi-Maskawa (CKM) matrix

In the SM, the 3×3 unitary CKM matrix [11, 12] describes quark mixing. The measurement of $|V_{tb}|$ is based on the relation $\mathcal{R} = \mathcal{B}(t \rightarrow Wb) / \sum_q \mathcal{B}(t \rightarrow Wq) = |V_{tb}|^2 / \sum_q |V_{tq}|^2$ where q is any down-type quark. Due to unitarity $\sum_q |V_{tq}|^2 = 1$ and thus $\mathcal{R} = |V_{tb}|^2$. A global fit in the SM gives $|V_{tb}| = 0.999146_{-0.000046}^{+0.000021}$ [107]. Any experimental deviation from this value will be evidence for new BSM physics, for example, existence of a fourth quark generation [158].

The results of \mathcal{R} measurements are summarized in Table 7. The channels of the $t\bar{t}$ events selected for analysis are ℓ +jets and dilepton in Ref. [133], ℓ +jets in Ref. [159], and dilepton in Refs. [160, 134]. When restricting to $\mathcal{R} \leq 1$, the $|V_{tb}|$ lower limit in Ref. [134] becomes 0.955. All results are consistent with SM expectations.

The value of $|V_{tb}|$ can also be obtained from the single top production cross sections without the assumption of three quark generations or the unitarity of the CKM matrix as discussed in Section 5.

8 Role of the top quark in the Standard Model

The top quark, as the weak isospin partner of the b -quark, plays an important role in the SM and in its predictions for experiments. Here we consider briefly several aspects of the role of top quarks: cancellations of chiral anomalies, flavor changing neutral currents and the GIM mechanism, the large top Yukawa coupling and consistency of the Higgs mechanism of spontaneous electroweak symmetry breaking [161, 162, 163, 164, 165], and large quantum corrections to electroweak observables.

8.1 Standard Model self-consistency: chiral anomalies.

The top quark is needed for the consistency of the SM as a gauge quantum field theory. In the SM, the fermions, both leptons and quarks, are combined into three

generations forming left-handed doublets and right-handed singlets with respect to the weak isospin $I_f^{L,R}$

$$I_f^{L,R} = \pm \frac{1}{2}, 0 : \begin{array}{l} \begin{pmatrix} \nu_e \\ e^- \end{pmatrix}_L, e_R^- \quad : \quad \begin{pmatrix} u \\ d \end{pmatrix}_L, u_R, d_R \\ \begin{pmatrix} \nu_\mu \\ \mu^- \end{pmatrix}_L, \mu_R^- \quad ; \quad \begin{pmatrix} c \\ s \end{pmatrix}_L, c_R, s_R \\ \begin{pmatrix} \nu_\tau \\ \tau^- \end{pmatrix}_L, \tau_R^- \quad : \quad \begin{pmatrix} t \\ b \end{pmatrix}_L, t_R, b_R \end{array}$$

where for any fermion field f the left and right chiral components are defined as

$$f_{L,R} = \frac{1}{2}(1 \mp \gamma_5)f$$

In order to correctly reproduce the electromagnetic and weak interactions, the gauge group of the electroweak part of the SM is taken as

$$SU_L(2) \otimes U_Y(1), \quad (2)$$

where $SU_L(2)$ is called the weak isospin group (the weak isospin is an analog of the usual isospin introduced by Heisenberg to describe the proton and the neutron) and $U_Y(1)$ is the weak hypercharge group. The hypercharges of the left- and right-handed lepton and quark fields are chosen such that the electric charges are equal to the known measured charges

$$\begin{aligned} Q_f &= (T_3^f)_L + \frac{Y_L^f}{2} \\ Q_f &= (T_3^f)_R + \frac{Y_R^f}{2} \end{aligned} \quad (3)$$

where $(T_3^f)_{L,R}$ are the isospin projections $+1/2$ for the up-type component and $-1/2$ for the down-type component of the fermions, $Y_{L,R}^f$ stands for corresponding weak hypercharges of the fermions. These relations are known as the Gell Mann – Nishijima formulas. The relations for the group generators guarantee that after the spontaneous symmetry breaking, the gauge symmetry $SU_L(2) \otimes U_Y(1)$ reduces to the unbroken electromagnetic group $U_{em}(1)$.

Because of this chiral structure of the SM, there is a potential “chiral” anomaly problem. Generically, anomalies in a field theory correspond to the situation where some symmetry is present at the level of a classical Lagrangian but is violated at the quantum loop level. Indeed, after a quantization of the SM one finds that the left- and right-handed fermion currents, conserved in accord with Noether theorem at the classical level, are not conserved for individual leptons or quarks at quantum level due to the triangle loop contributions shown in Fig. 17.

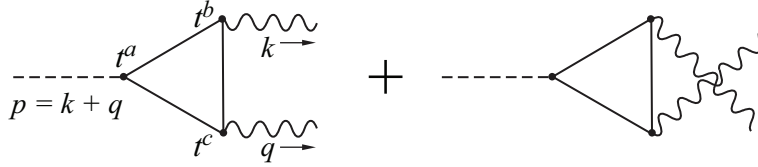


Figure 17: Loop corrections leading to anomalies. p, q, k are 4-momenta and t^a, t^b, t^c are a generic notation for the gauge group generator in the interaction vertex of corresponding gauge boson with the fermion in the loop.

If an anomaly does not vanish, the theory loses its gauge invariance and therefore cannot be acceptable. (However, in the case of anomaly free fundamental theories such as QED one may consider some currents, for example pseudoscalar fermion pair currents, that respect some global symmetry at the classical level in addition to the local gauge symmetries of the fundamental theory. Anomalies for such currents do not lead to problems. Moreover, this type of anomaly may have very important physics consequences, as in the case of π^0 decay to two photons.) In the SM there are simultaneous contributions from left and right chiral fermions which contribute to the anomaly with opposite signs. The anomaly is then proportional to the differences between traces of group generators coming from fermions with left and right chiralities:

$$\text{Anomaly} \sim \text{Tr} [t^a \{t^b t^c\}]_L - \text{Tr} [t^a \{t^b t^c\}]_R, \quad (4)$$

where the square and the curly brackets denote commutators and anticommutators respectively.

In theories like QED or QCD there are no γ_5 matrices in the Lagrangians. Therefore the left and right chiral contributions exactly compensate each other, so the anomaly is equal to zero and the theories make perfect sense.

In the electroweak part of the SM, left- and right-handed states couple to $U_Y(1)$ gauge bosons with different hypercharges, and only the left components couple to the $SU_L(2)$ gauge bosons. So, it is not obvious *a priori* that the chiral anomalies vanish. But the absence of anomalies is a requirement for the SM to be a valid quantum theory.

Without going into details (they can be found in textbooks, see e.g. [166], [167], [168]) one can check that all the chiral anomalies are canceled in the SM for each fermion generation due to the simultaneous contributions of quarks and leptons with left and right chiralities. In particular, the cancellation of the anomaly in each generation takes place due to the sum of electric charges of leptons being equal in magnitude but opposite in sign to the sum of quark charges. For such a cancellation, the number of colors (N_c) must be equal to three. In particular, the

cancellation for the third generation requires a top quark with charge $Q_t = +2/3$, giving $(Q_t + Q_b) \times N_c + Q_\tau = 0$.

8.2 Flavor changing neutral currents and the GIM mechanism.

The basic principle in constructing the SM Lagrangian is gauge invariance, which allows us to consider only two types of gauge invariant terms containing quark-Higgs Yukawa interactions with mixing of the down- and up-type quark fields from different generations:

$$L_{\text{Yukawa}} = -\Gamma_d^{ij} \bar{Q}'_L{}^i \Phi d'_R{}^j - \Gamma_u^{ij} \bar{Q}'_L{}^i \Phi^C u'_R{}^j + h.c. , \quad (5)$$

where $\Gamma_{u,d}^{ij}$ are generic mixing coefficients, $Q'_L = \begin{pmatrix} u' \\ d' \end{pmatrix}_L$ with the symbol $(')$ used to account for quark states before rotation to the mass eigenstates, and the Higgs Φ and conjugated Higgs Φ^C fields in the unitary gauge have the forms

$\Phi = \frac{1}{\sqrt{2}} \begin{pmatrix} 0 \\ v+h \end{pmatrix}$, $\Phi^C = \frac{1}{\sqrt{2}} \begin{pmatrix} v+h \\ 0 \end{pmatrix}$, where $v = 246$ GeV is the vacuum expectation value and h is the scalar Higgs boson.

After spontaneous symmetry breaking the Lagrangian (5) takes the form

$$L_{\text{Yukawa}} = - \left[M_d^{ij} \bar{d}'_L{}^i d'_R{}^j + M_u^{ij} \bar{u}'_L{}^i u'_R{}^j + h.c. \right] (1 + h/v)$$

where $M^{ij} = \Gamma^{ij} v / \sqrt{2}$ are mass mixing matrices for down- and up-type quarks. The matrices should be diagonalized to get the physical states for up- and down-type quarks. This can be done using unitary transformations in flavor space for all types of up and down, left and right quark fields

$$d'_{Li} = (U_L^d)_{ij} d_{Lj}; \quad d'_{Ri} = (U_R^d)_{ij} d_{Rj}; \quad u'_{Li} = (U_L^u)_{ij} u_{Lj}; \quad u'_{Ri} = (U_R^u)_{ij} u_{Rj}$$

After such transformations the above Yukawa Lagrangian contains Dirac mass terms for quarks and their interactions with the Higgs boson are proportional to the fermion masses:

$$L_{\text{Yukawa}} = - \sum_{i=1}^3 [m_d^i \bar{d}^i d^i + m_u^i \bar{u}^i u^i] \left(1 + \frac{h}{v}\right), \quad (6)$$

where $i = 1, 2, 3$ stands for three flavor generations, and in particular, m_u^3 is the top quark mass m_t .

Recall that in the SM all fermion interactions with vector gauge fields follow from the gauge invariance principle and are expressed in terms of the products of

the gauge fields to neutral and charge currents containing fermions from the same generation. Therefore the above unitary transformations ($U^\dagger U = 1$) do not affect the neutral currents. As a result there are no flavor changing neutral currents in the SM at lowest order.

However, the charge currents

$$J_C^\mu \sim \bar{u}'_L \gamma^\mu d'_L + h.c.$$

contain quarks rotated by different unitary matrices for the up- and down-type quarks

$$u' \rightarrow (U_L^u)u, \quad d' \rightarrow (U_L^d)d.$$

Therefore after the unitary transformation the charge current becomes:

$$J_C^\mu \sim (U_L^u)^\dagger U_L^d \bar{u}_L \gamma^\mu d_L.$$

The unitary matrix

$$V_{CKM} = (U_L^u)^\dagger U_L^d$$

is called Cabbibo-Kobayashi-Maskawa mixing matrix [11, 12]:

$$V_{CKM} = \begin{pmatrix} V_{ud} & V_{us} & V_{ub} \\ V_{cd} & V_{cs} & V_{cb} \\ V_{td} & V_{ts} & V_{tb} \end{pmatrix} \quad (7)$$

The CKM matrix is unitary since it is constructed from the product of unitary matrices. However this is true only because of the presence of the top quark in the third generation.

The unitarity leads to various constraints on the elements of the CKM matrix such as

$$\sum_{k=1}^{k=3} V_{ik}^\dagger V_{kj} = \delta_{ij}.$$

One of the consequences of such unitary constraints is the GIM mechanism, formulated originally for the case of two generations [7] but with obvious extension to three generations. The GIM mechanism allows one to understand flavour changing neutral current (FCNC) suppression at higher orders of perturbation theory in the SM. As explained above, the FCNC are absent in the SM at the lowest order by construction. However, at higher orders the FCNC appear in the case of two (real or virtual) W^+ and W^- emissions by the quark current. For example, the FCNC $b \rightarrow s$ transition is proportional to

$$V_{su}^\dagger V_{ub} S(p, m_u) + V_{sc}^\dagger V_{cb} S(p, m_c) + V_{st}^\dagger V_{tb} S(p, m_t)$$

where $S(p, M_{u,c,t})$ is the propagator of the corresponding up-type quark with a momentum p . In the case of equal quark masses one would have the factor

$$V_{su}^\dagger V_{ub} + V_{sc}^\dagger V_{cb} + V_{st}^\dagger V_{tb}$$

in front of the current, which is equal to zero due to the unitary constraint. This is the exact GIM cancellation. If quark masses are not equal, as happens in nature, the FCNC will be non-zero and will give well defined predictions for various phenomena in physics of kaons, D and B mesons such as oscillations, rare decays, etc. An example is the rare decay of the B_s meson to a muon pair $\mu^+\mu^-$. Due

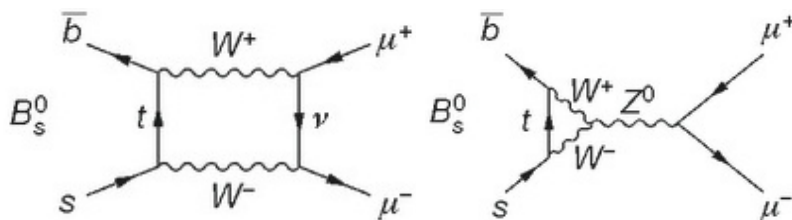


Figure 18: Box and Penguin loop diagrams contributing to the rare decay $B_s \rightarrow \mu^+\mu^-$.

to absence of the FCNC at tree level the leading Feynman diagrams are the loop diagrams, called box and penguin, as shown in Fig.18. In this case the diagrams involving virtual top quark dominate and lead to a theoretical decay rate in the SM of $\mathcal{B}(B_s \rightarrow \mu^+\mu^-) = (3.66 \pm 0.23) \times 10^{-9}$ [169], in good agreement with measured values by the LHCb [170] and the CMS [171] experiments.

We stress that the GIM mechanism works for three fermion generations only because of existence of the top quark.

8.3 Top quark Yukawa coupling and consistency of the SM at high energy scales.

As follows from the Lagrangian (6), the Yukawa top-Higgs interaction is proportional to the top quark mass

$$L_{t-h} = -\frac{m_t}{v} \bar{t} t h \quad (8)$$

and therefore it is strong since the top quark mass is large. The top Yukawa coupling

$$y_t = \frac{\sqrt{2}m_t}{v} \quad (9)$$

is numerically close to unity. Such a large top Yukawa coupling makes a significant impact on the Higgs potential when higher order corrections are considered.

In the SM, as for any quantum field theory, all the masses and coupling constants get quantum corrections and become so-called running masses and running coupling constants. In particular, the Higgs boson self-interaction quartic coupling λ gets loop corrections coming from the top, Higgs and electroweak gauge boson loops. As a result of the renormalization group evolution, λ becomes a function of the energy scale (renormalization scale μ). The analyses of the running coupling are performed at NNLO accuracy [172], [173], [174]. Because of the running of the Higgs self-coupling, the behavior of the Higgs potential may be changed drastically at high energy scales. Since the effective Higgs potential is proportional to $\lambda(\mu)$ at large μ or equivalently at large value of the Higgs field, different situations may occur. The quartic coupling $\lambda(\mu)$ may be positive all the way up to the Planck scale leading to an absolutely stable theory. On the other hand, $\lambda(\mu)$ may become negative at large μ , leading to a potential that falls with μ leading to instability of the theory. Or $\lambda(\mu)$ may take such values that a second minimum of the potential appears at some particular scale, leading to metastability due to possible tunneling effects.

The second minimum takes place at some scale μ_0 where the derivative of $\lambda(\mu)$, or equivalently the β function, is zero

$$\beta(\mu) = \frac{d}{d \ln(\mu)} \lambda(\mu) = 0, \quad \text{at } \mu = \mu_0. \quad (10)$$

If the value of the potential at the new minimum μ_0 is less than the value of the vacuum potential at the electroweak scale then the theory is metastable. The boundary between stable and meta-stable cases corresponds to a situation where the first and second minima of the potential are equal. The minimum can always be chosen to be zero by a constant shift of the potential. This is equivalent to the condition

$$\lambda(\mu_0) = 0 \quad (11)$$

at some scale called the critical point $\mu_0 = M_{crit}$.

Because the largest loop corrections in the evolution of $\lambda(\mu)$ are proportional to various powers of the top Yukawa coupling y_t , the accuracy of the top quark mass measurement is of special importance. Results of the NNLO analysis are shown in Fig.19 [174]. As one can see, given the uncertainties, the second minimum and critical point could be achieved at the Planck scale. However, a top quark mass of about 171.3 GeV is needed for this to occur. If the top quark mass is heavier, the quartic coupling crosses zero at lower μ . In particular, the value of the top quark mass close to the current measured value $m_t = 173.1 \pm 0.6$ GeV leads to the scale $\mu \sim 10^{10}$ GeV for which the quartic coupling becomes negative.

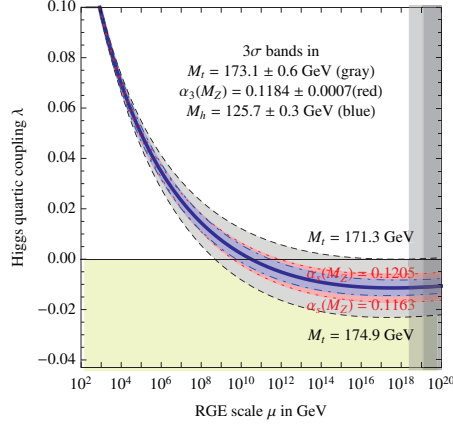


Figure 19: Renormalization group evolution of λ varying M_{top} , M_h and α_s by $\pm 3\sigma$ [174].

Keeping in mind the relation between the Higgs mass and the quartic coupling $M_h^2 = 2\lambda v^2$, a bound is obtained for the Higgs mass, assuming the critical point to be the Planck scale [174]

$$M_h \text{ [GeV]} > 129.4 + 1.4 \left(\frac{m_t \text{ [GeV]} - 173.1}{0.7} \right) - 0.5 \left(\frac{\alpha_s(M_Z) - 0.1184}{0.0007} \right) \pm 1.0_{\text{th}} , \quad (12)$$

where $\alpha_s(M_Z)$ is the running QCD coupling constant taken at the Z -boson mass M_Z , and 1.0_{th} GeV is an estimation of theoretical uncertainty of all involved loop computations. If one combines in quadrature the theoretical uncertainty and the experimental uncertainties on m_t and α_s one gets $M_h > 129.4 \pm 1.8$ GeV. Therefore the conclusion from this analysis is that the stability of the SM vacuum up to the Planck scale is excluded for $M_h < 126$ GeV at 98% CL.

If one solves the system of critical equations (10) and (11), one finds boundaries for ranges of stability, meta-stability and instability [174, 175, 176]. The result from Ref. [174] is shown in Fig. 20. The area defined by the current measured values and uncertainties of $\alpha_s(M_Z)$, m_t and M_H is located in the metastability region, but close to the boundary with the stability region. However, the lifetime of such a metastable vacuum is estimated to be much larger than the current age of the Universe.

The exclusion of the SM as a valid quantum theory up to the Planck scale is only at the 2 sigma level with today's measured top quark and Higgs boson masses, so one can not fully reject the hypothesis that the SM works all the way up to the Planck scale. This allows one to consider scenarios with the SM Higgs acting as an inflaton [177, 178]. Clearly, a better precision of the top quark mass is

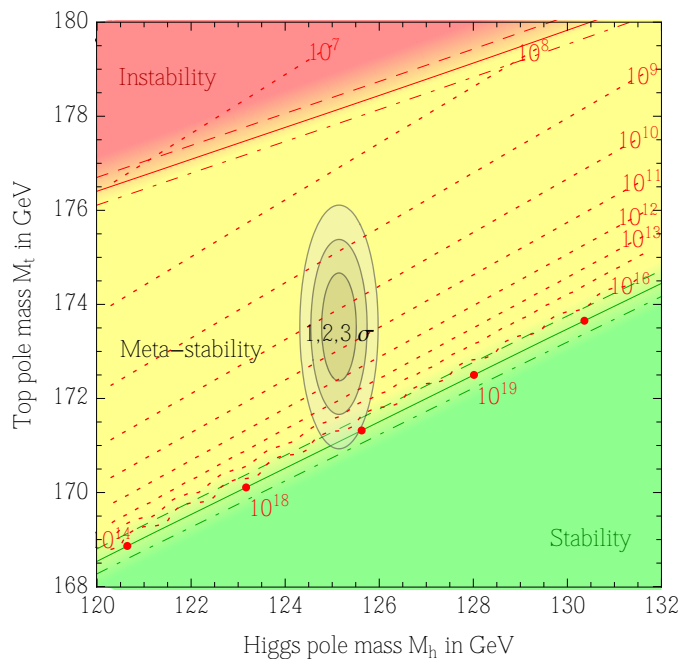


Figure 20: Regions of stability, meta-stability and instability of the SM vacuum in the M_t – M_h plane close to the experimentally allowed range of M_h and M_t at 1, 2, and 3σ . Boundary lines correspond to $\alpha_s(M_Z) = 0.1184 \pm 0.0007$ [174].

needed as may be achieved at the LHC, but certainly at a future e^+e^- collider. As the precision of the top quark mass measurement becomes substantially smaller than 1 GeV, it will become imperative that the measured mass has a well defined theoretical meaning (see Section 6). Also, to discriminate between stability, metastability or criticality of the electroweak vacuum, a contribution from possible “new physics” might be very essential [18, 179].

A large top mass and correspondingly large top Yukawa coupling lead to a potential problem of the SM called “naturalness” or the “hierarchy” problem. The loop corrections to the Higgs boson mass shown in Fig. 21 give the following leading expression

$$\delta M_h^2 = \frac{3G_F}{4\sqrt{2}\pi^2} (2M_W^2 + M_Z^2 + M_h^2 - 4M_{top}^2) \Lambda^2 \approx -(0.2\Lambda)^2, \quad (13)$$

where the cutoff parameter Λ represents the possible “new physics” scale. The main contribution to the correction comes from the top quark loop.

The problem is that the correction depends very strongly (quadratically) on the scale Λ which may be related to contributions from “new physics”. If Λ is very large, (e.g. the Planck scale or even 10^{10} GeV), the Higgs mass of the order of

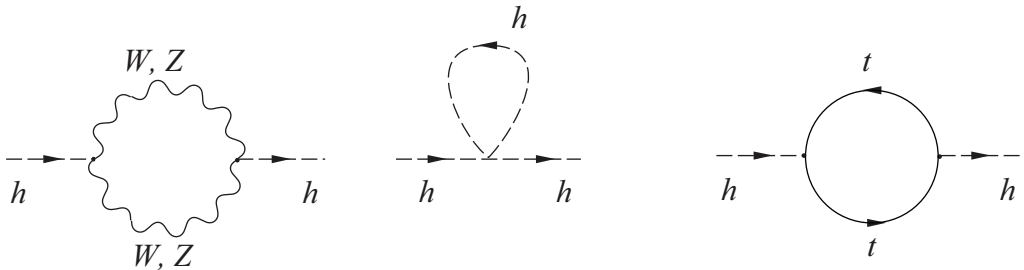


Figure 21: Loops contributing to the Higgs mass correction.

100 GeV is very unnatural. Such a dependence is a specific property of the scalar Higgs boson. Quadratic scale dependences for other SM particles are protected by a symmetry – gauge symmetry for the gauge bosons and chiral symmetry for fermions, but there is no such SM symmetry protecting Higgs quadratic dependence. If one requires the correction to the Higgs mass to be less than the Higgs mass itself, $\delta M_h < M_h$, one finds the upper limit on the scale Λ to be slightly less than 1 TeV (the “little hierarchy” problem). No new physics particles at this mass scale have been found yet. But since the main contribution to the Higgs mass correction comes from the top loop, one might expect the existence of some rather light top-quark partners, such as stop quarks in supersymmetric models, giving additional loop contributions which may cancel the top loop quadratic behavior on Λ [180, 181, 182, 183].

8.4 Quantum corrections to electroweak observables

Because of the large top quark mass, one naively would think that the loop contributions from such a heavy particle would be suppressed. Indeed, in theories like QED or QCD the top quark loop contributions are much smaller than those from light quarks. However, this is not true for the electroweak part of the SM. In previous sections we have seen that due to the large top Yukawa coupling, top loops are very important. For example, the main Higgs boson production channel at the Tevatron or LHC, gluon-gluon fusion, proceeds mainly through a top quark triangle diagram. Also, in the SM the masses of the electroweak gauge bosons W^\pm and Z appear due to the Higgs mechanism of spontaneous symmetry breaking, and the longitudinal component of the massive vector boson fields come from would-be Goldstone bosons. In the unitary gauge the Goldstone bosons are “eaten” by the longitudinal modes. Loop corrections to the electroweak observables are computed in covariant gauges where the interaction vertices of the Goldstone bosons with quarks are involved. These vertices contain terms proportional to the fermion masses, and therefore the loops containing the top quark give the largest contribu-

tions. As an example, the loop correction to the W boson mass shown in Fig. 22 due to top quarks depends quadratically on the top mass, while the Higgs boson



Figure 22: Loop corrections to the W boson mass involving the top quark and the Higgs boson.

loop correction depends logarithmically on the Higgs mass. Analysis of these mass corrections provided important limits on the Higgs mass [184] prior to the Higgs discovery by confronting the measured m_t and M_W with the calculations including these loop corrections, as shown in Fig. 23. These limits pointed to the region where the Higgs was subsequently discovered at the LHC [185, 186].

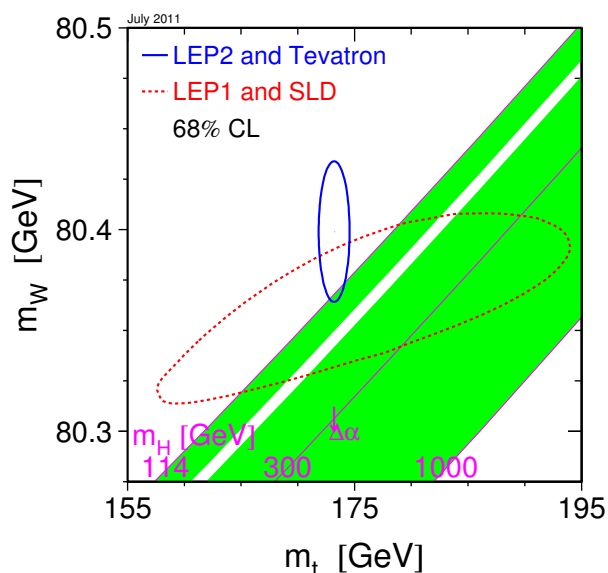


Figure 23: W boson mass as a function of the top quark mass at various values of the Higgs mass and the constraint on potential Higgs masses prior to the Higgs discovery. The open band around $M_H = 160$ GeV had been excluded by the Tevatron experiments.

The plot in the $M_W - m_t$ plane from the global fit of precision electroweak measurements by the SM loop level predictions [17] is shown in Fig. 24. The

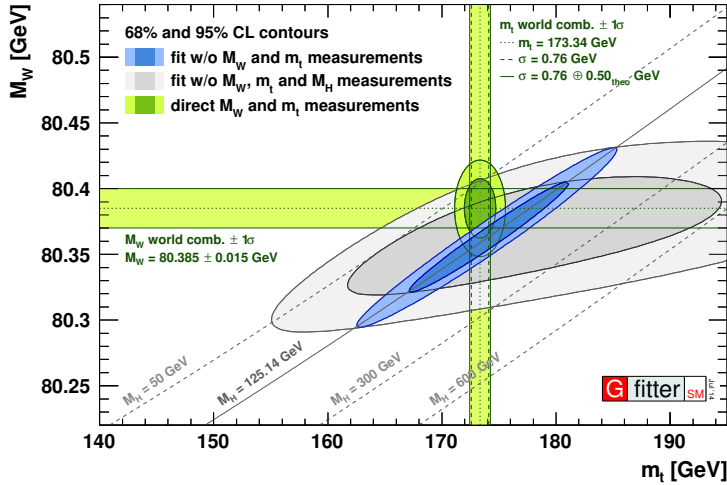


Figure 24: Two dimensional plot for W -boson and top quark masses from the global fit of precision electroweak data excluding (grey area) and including (blue area) the Higgs mass measurements, to be compared with the directly measured values for the masses indicated by the horizontal and vertical bands.

narrower blue and larger grey areas allowed at 1 and 2σ correspond to the cases when measurements of the Higgs boson mass are included or excluded in the fit. These fits do not include the experimental M_W and m_t constraints. The allowed regions coincide well with the vertical and horizontal bands indicating the 1σ regions for the m_t and M_W direct measurements.

There are many other cases where the top loop contributions are large; for example, the partial decay width of the Z boson to the $b\bar{b}$ -quark pair.

9 Top quark as a window to new physics

The top quark is the heaviest particle of the SM, which suggests that it may play a special role in the EW symmetry breaking (cf. Section 8). It also plays a central role in many Beyond the Standard Model (BSM) scenarios. This suggests the use of signatures in the production of pairs or single top quarks to search for such BSM scenarios. In this Section, we review the latest experimental results using the top quark as a window to BSM physics.

9.1 Searches for associated $t\bar{t}H$ production

In the SM, the top quark Yukawa coupling y_t is numerically within 1% of unity given the world average value of $m_t = 173.34 \pm 0.76$ GeV [10]. A significant

deviation of y_t from $y_t^{\text{SM}} \approx 1$ would be a clear indication of BSM phenomena. With the recent addition of the Higgs boson to the family of known particles, it is therefore imperative to measure y_t directly, which can be accomplished using the associated production of a Higgs boson and a $t\bar{t}$ pair, where the Higgs boson is identified through the $H \rightarrow b\bar{b}$, $H \rightarrow \gamma\gamma$, $H \rightarrow WW$ or $H \rightarrow ZZ$ decay modes. The first search for $t\bar{t}H(b\bar{b})$ production at a hadron collider was carried out in 2009 by D0 using 2.1 fb^{-1} of data [187]. The best observed (expected) limit at the Tevatron for $t\bar{t}H(b\bar{b})$ is $\mu < 17.6$ (12.4) in units of the SM expected cross section at 95% CL assuming $M_H = 125 \text{ GeV}$, obtained by CDF using 9.4 fb^{-1} of data [188]. The best limits at the LHC come from ATLAS and CMS collaborations, both in the $t\bar{t}H(b\bar{b})$ mode. The ATLAS analysis applies a neural network discriminant and a ME method to 20.3 fb^{-1} of data in the ℓ +jets and dilepton channels, and obtains an observed (expected) upper limit of $\mu < 3.4$ (2.2) at 95% CL [189]. Similarly, the CMS analysis obtains an observed (expected) limit of $\mu < 4.2$ (3.3) at 95% CL by applying a ME method to 19.5 fb^{-1} of data in the ℓ +jets and dilepton channels [190]. The results correspond to a fitted $\mu = 1.5 \pm 1.1$ for ATLAS and 1.2 ± 1.6 for CMS, consistent with the SM y_t value.

9.2 Searches for non-SM Higgs bosons

Many BSM models such as supersymmetry (see Section 9.3) predict an extended Higgs boson sector. The simplest extension, the 2 Higgs Doublet Model (2HDM) [191], postulates two complex $\text{SU}(2)_L$ doublet scalar fields rather than one in the SM. This results in eight degrees of freedom, three of which give masses to the SM W and Z bosons, while five manifest themselves as physical particles: two neutral scalars h and H , one pseudoscalar A , and two charged scalars H^\pm . Typically, h is assumed to correspond to the discovered Higgs boson. An important parameter of 2HDM models is the ratio $\tan\beta$ of the vacuum expectation values of the two $\text{SU}(2)_L$ doublets. Large $\tan\beta$ results in enhanced couplings to third generation fermions of the SM. The couplings of H^\pm bosons to SM particles are dominated by the $H^+t\bar{b}$ (and charge conjugate) vertex due to the large top quark mass. Hence, searches for H^\pm bosons concentrate on the $H^+ \rightarrow t\bar{b}$ process if $M_{H^\pm} > m_t$, and on $t \rightarrow H^+b$ if $M_{H^\pm} < m_t$.

The first search for $H^+ \rightarrow t\bar{b}$ was carried out by D0 using the s -channel single top-like process $p\bar{p} \rightarrow H^+ \rightarrow t\bar{b} \rightarrow W^+b\bar{b}$ in 0.9 fb^{-1} of data [192]. Due to limited sensitivity, models with $\tan\beta < 100$ could not be excluded. CMS searched for $H^+ \rightarrow t\bar{b}$ through processes $pp \rightarrow H^+t\bar{b} \rightarrow \tau^+\nu\mu^+\nu\bar{b}b$ and $pp \rightarrow H^+t\bar{b} \rightarrow \ell^+\nu\bar{b}b\ell'^-\nu\bar{b}b$ using 19.5 fb^{-1} of data [193], and upper limits in the range $180 \text{ GeV} < m_{H^\pm} < 600 \text{ GeV}$ for $\tan\beta = 30$ have been placed.

Large values of $\tan\beta$ make the $H^+ \rightarrow \tau^+\nu$ decay mode favourable for $t \rightarrow H^+b$ searches, where the τ lepton is typically identified through its hadronic decays.

CDF searched for $H^+ \rightarrow \tau^+\nu$ decays in $t\bar{t}$ -like topologies in the ℓ +jets and $\ell\ell$ channels through an enhancement of events with τ leptons using 0.2 fb^{-1} of data [194]. Similar searches were performed by D0 in the $\ell\ell$ channel using 0.9 fb^{-1} of data [195] and in the ℓ +jets and $\ell\ell$ channels using 1 fb^{-1} of data [196]. Following the same strategy, ATLAS and CMS carried out searches for $t \rightarrow H^+b$ using 19.5 fb^{-1} [197] and 19.7 fb^{-1} of data [198] at $\sqrt{s} = 8 \text{ TeV}$ in ℓ +jets and $\ell\ell$ channels, respectively. In the absence of BSM signal, upper limits on $\mathcal{B}(t \rightarrow H^+b) \times \mathcal{B}(H^+ \rightarrow \tau^+\nu)$ were placed in the $(M_{H^\pm}, \tan\beta)$ -plane down to $M_{H^\pm} = 80 \text{ GeV}$.

The $H^+ \rightarrow c\bar{s}$ decay mode is favourable for small values of $\tan\beta$. The first search for this decay mode was carried out by CDF in $t\bar{t}$ -like events in the ℓ +jets channel, where the invariant mass of the non- b -tagged dijet system was used to discriminate $t \rightarrow H^+b$ against SM $t \rightarrow W^+b$ decays [199]. The same strategy was pursued by ATLAS using 4.7 fb^{-1} of data at $\sqrt{s} = 7 \text{ TeV}$ [200] and by CMS with 19.7 fb^{-1} at $\sqrt{s} = 8 \text{ TeV}$ [201]. D0 performed a simultaneous search for the $H^+ \rightarrow c\bar{s}$ and $H^+ \rightarrow \tau^+\nu$ decay modes by analysing the ℓ +jets and $\ell\ell$ channels divided into regions according to the multiplicity of identified b -quark jets, using both hadronic and leptonic τ decays [202]. In absence of BSM signal, upper limits on $\mathcal{B}(t \rightarrow H^+b) \times \mathcal{B}(H^+ \rightarrow c\bar{s})$ were placed in the $(M_{H^\pm}, \tan\beta)$ -plane for $80 \text{ GeV} < M_{H^\pm} < 160 \text{ GeV}$.

9.3 Searches for supersymmetric partners of the top quark

Supersymmetry [203] is widely considered to be a promising model for the extension of the SM. Its simplest version postulates a supersymmetric bosonic partner \tilde{f} for each SM fermion f . A wide class of supersymmetric models predicts a natural dark matter candidate, which is typically the lightest neutralino mass eigenstate $\tilde{\chi}_1^0$ [203]. In the SM, M_H receives loop contributions from each of the SM fermions which can be orders of magnitude larger than M_H itself (cf. Section 8). This fine-tuning problem, also known as the hierarchy problem, can be elegantly resolved in supersymmetry, where the loop contribution of each f is cancelled by its superpartner \tilde{f} . The top quark contribution to M_H is largest due to $m_t \gg m_{f \neq t}$, hence models with stop mass eigenstates \tilde{t}_1 and \tilde{t}_2 that are much lighter than all other \tilde{f} and with $m_{\tilde{t}_1} \approx m_t$ are preferred, suggesting searches for supersymmetry through top quarks.

Assuming that \tilde{t}_1 is the next-to-lightest and $\tilde{\chi}_1^0$ the lightest supersymmetric particle which is stable, three phase space regions with distinct decay modes can be identified as: (i) $M_{\tilde{t}_1} - m_{\tilde{\chi}_1^0} > m_t$ with $\tilde{t}_1 \rightarrow t\tilde{\chi}_1^0$; (ii) $M_W + m_b < M_{\tilde{t}_1} - m_{\tilde{\chi}_1^0} < m_t$ with $\tilde{t}_1 \rightarrow Wb\tilde{\chi}_1^0$; and (iii) $M_{\tilde{t}_1} - m_{\tilde{\chi}_1^0} < M_W + m_b$ with $\tilde{t}_1 \rightarrow bW^*\tilde{\chi}_1^0$ where W^* is an off-shell W boson, or $\tilde{t}_1 \rightarrow c\tilde{\chi}_1^0$ via loop-suppressed diagrams.

Many searches for supersymmetry at the Tevatron focused on the extended

Higgs sector, which in many supersymmetric scenarios corresponds to that of 2HDM models summarised in Section 9.2. Beyond this, CDF searched for pair-produced stops with $\tilde{t}_1 \rightarrow b\tilde{\chi}_1^\pm \rightarrow b\tilde{\chi}_1^0 W^{(*)}$ [204].

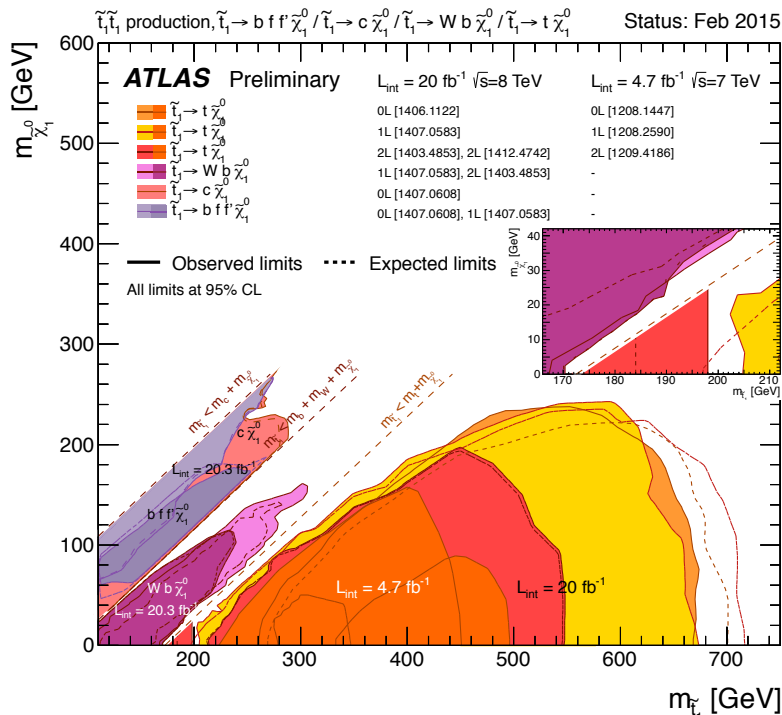


Figure 25: Overview of the ATLAS search results [205] for direct stop pair-production for scenarios where no other supersymmetric particles besides \tilde{t}_1 and $\tilde{\chi}_1^0$ are involved in the \tilde{t}_1 decays. Observed (expected) exclusion limits at 95% CL are shown as solid (dashed) lines in the $(M_{\tilde{t}_1}, m_{\tilde{\chi}_1^0})$ plane. The diagonal dashed lines indicate the three kinematic regimes (i)-(iii) discussed in the text, where different decay modes are considered with $\mathcal{B} = 100\%$.

Decays in all three $M_{\tilde{t}_1}$ regions (i)-(iii) were used to search for supersymmetry by ATLAS and CMS. A summary of the exclusion 95% CL limits by ATLAS using up to 20 fb^{-1} of data at $\sqrt{s} = 8 \text{ TeV}$ and 4.7 fb^{-1} at $\sqrt{s} = 7 \text{ TeV}$ is shown in Fig. 25. A substantial part of the $(M_{\tilde{t}_1}, m_{\tilde{\chi}_1^0})$ plane is experimentally excluded, and the different decay modes are covered by complementary analyses reviewed in Ref. [205]. The exclusion sensitivity at high $M_{\tilde{t}_1}$ is driven by analyses exploiting boosted topologies and jet substructure techniques in the $\ell + \text{jets}$ and all-jets channels. It extends to $M_{\tilde{t}_1} \approx 700 \text{ GeV}$ and is limited by $\sigma_{\tilde{t}_1 \tilde{t}_1}$ in both channels. The intermediate kinematic regions at constant $M_{\tilde{t}_1} - m_{\tilde{\chi}_1^0}$ indicated by the dashed lines in Fig. 25 are experimentally challenging due to the similarity of the resulting signatures to those from SM processes. These regions are addressed

by precision measurements of $\sigma_{t\bar{t}}$ in the $e\mu$ channel at $\sqrt{s} = 7$ TeV and $\sqrt{s} = 8$ TeV with an experimental uncertainty of about 4% [124], and by a measurement of the correlations between the spins of the t and \bar{t} quarks [206]. The exclusion limits by CMS are similar to those shown in Fig. 25, and come from Refs. [207, 208, 209, 210, 211].

An alternative strategy employed both by ATLAS and CMS is to search for the heavier stop mass eigenstate \tilde{t}_2 which then decays to \tilde{t}_1 [212, 213]. In the absence of signal, exclusion limits are set in the $(M_{\tilde{t}_1}, M_{\tilde{t}_2})$ plane up to (450 GeV, 600 GeV). In addition, a \tilde{t}_1 signal was searched for in pair-production of gluinos \tilde{g} , the superpartner of the gluon, by both ATLAS and CMS [214, 215], and exclusion limits are set in the $(M_{\tilde{t}_1}, m_{\tilde{g}})$ plane up to (700 GeV, 1400 GeV).

9.4 Searches for vector-like quarks

Vector-like quarks (VLQ) have been proposed in many BSM scenarios such as composite Higgs [216, 217, 218] and little Higgs models [219, 220, 221, 222], mainly motivated to address the naturalness problem. VLQs are defined as quarks with left- and right-handed components transforming identically under $SU(2)_L$. Models with weak isospin singlets, doublets, and triplets have been proposed, where in the doublet case VLQs can occur as up-type quarks (T) or down-type quarks (B). VLQs predominantly decay to third generation quarks and produce signatures either involving top quarks or resembling them. Typical discrimination variables are H_T , defined as the scalar sum of the transverse momenta of all jets and possibly leptons, and the mass of the T , m_T , determined through a kinematic fit.

At the Tevatron, searches focus on pair-produced VLQs which decay as $B \rightarrow Wt$ or $T \rightarrow Wb$. CDF searched for $T\bar{T}$ production in the $\ell + \text{jets}$ channel using 5.6 fb^{-1} of data, and excluded $m_T < 360$ GeV at 95% CL [223]. The exclusion of $m_T < 285$ GeV from D0 using 5.3 fb^{-1} of data [224] is weaker due to a 2.5σ excess in the $\mu + \text{jets}$ channel. CDF excluded $m_B < 370$ GeV searching for $B\bar{B}$ production in 4.8 fb^{-1} of data [225].

Similar search strategies are employed at the LHC, however the potential decay modes are extended to $B \rightarrow Wt, Zb, Hb$ and $T \rightarrow Wb, Zt, Ht$, and some searches target the production of single VLQs. In some cases, signatures with same-sign leptons are used. In addition, for VLQ masses above about 500 GeV, boosted signatures and jet-substructure techniques (cf. Section 9.5) are applied. In the absence of signal, $m_T < 750$ GeV (900 GeV) are excluded at 95% CL for $\mathcal{B}(T \rightarrow Ht) = 1$ ($\mathcal{B}(T \rightarrow Ht) = 0$) by ATLAS [226, 227, 228] and $m_T < 650$ GeV (800 GeV) by CMS [229, 230, 231, 232, 233]. Similarly, $m_B < 600$ GeV (800 GeV) are excluded at 95% CL for $\mathcal{B}(B \rightarrow Hb) = 1$ ($\mathcal{B}(B \rightarrow Hb) = 0$) by ATLAS [226, 227, 228, 234] and $m_B < 550$ GeV (750 GeV) by CMS [229, 230].

9.5 Searches for new gauge bosons

An extended gauge sector with massive gauge bosons, generically denoted as W' or Z' , is predicted in many BSM scenarios such as the Arkani-Hamed, Dimopoulos, Dvali model with large extra dimensions [235] or the Randall-Sundrum model with warped extra dimensions [236, 237], and many others.

Assuming that the W' has SM-like $V - A$ couplings, searches with $W' \rightarrow \ell\nu$ provide the best sensitivity. However, if the W' couples only to right-handed particles and if hypothetical right-handed neutrinos are more massive than the W' , $W' \rightarrow t\bar{b}$ becomes the preferred search channel. Searches have also been performed for a leptophobic W' boson with left-handed couplings. Typically, search strategies concentrate on single top-like $t\bar{b}$ production through the s -channel, and use the invariant mass distribution of the $t\bar{b}$ system as a discriminant. The first W' search with arbitrary couplings was performed by D0 using 2.3 fb^{-1} of data [238], and $M_{W'} < 800 \text{ GeV}$ with purely left- or right-handed couplings were excluded. CDF excluded $M_{W'} < 900 \text{ GeV}$ with purely right-handed couplings using 9.5 fb^{-1} of data as shown in Fig. 26(a), and provides the world's most stringent limits on W' with $M_{W'} < 600 \text{ GeV}$ to date [239]. Similar search strategies were applied by the ATLAS and CMS collaborations to 20.3 fb^{-1} and 19.5 fb^{-1} of data, resulting in observed (expected) exclusion limits of $M_{W'} < 1.92 \text{ TeV}$ (1.75 TeV) [240] and $M_{W'} < 2.05 \text{ TeV}$ (2.02 TeV) [241], respectively, for a W' boson with purely right-handed couplings.

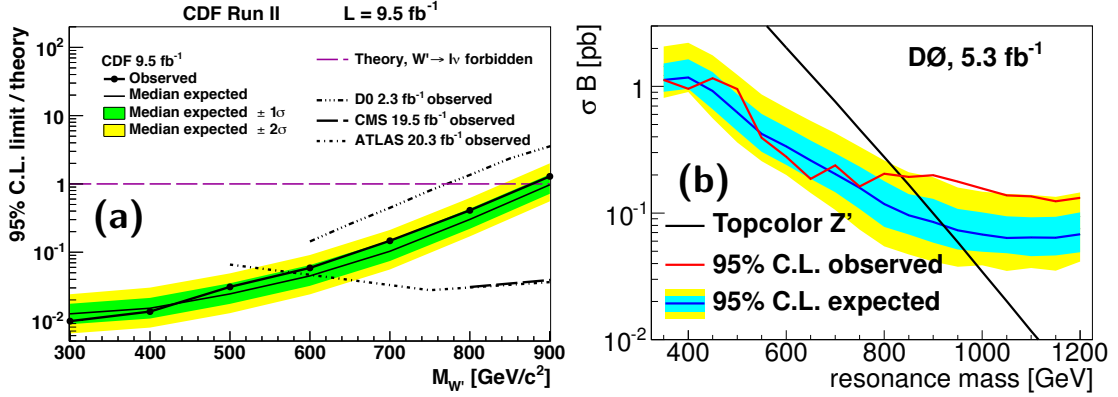


Figure 26: (a) Observed and expected upper limits on $\sigma_{W'} \times \mathcal{B}(W' \rightarrow t\bar{b})$ [239] at 95% CL are compared to theory predictions for a right-handed W' boson with SM-like coupling strengths. The exclusion limits by D0 [238], ATLAS [240], and CMS [241] are also shown. (b) Observed and expected upper limits on $\sigma_{Z'} \times \mathcal{B}(Z' \rightarrow t\bar{t})$ of a narrow topcolor Z' resonance [243] at 95% CL are compared to theory predictions as a function of $M_{Z'}$. The shaded regions around the expected limit represent the ± 1 and $\pm 2\sigma$ bands in (a) and (b).

Searches for $Z' \rightarrow t\bar{t}$ are performed following the classical bump-hunt strategy in the invariant mass spectrum of the $t\bar{t}$ system, for two generic scenarios: a resonance that is narrow relative to the detector resolution $\Gamma_{Z'}/m_{Z'} \approx 1\%$, representative of models such as topcolor [242]; and a broad resonance $\Gamma_{Z'}/m_{Z'} = 10 - 15\%$ as found for example in Randall-Sundrum model with warped extra dimensions. In 2012, the search for Z' resonances using 5.3 fb^{-1} of data [243] by D0 sparked some interest with an excess of 2σ at $m_{t\bar{t}} \approx 1 \text{ TeV}$, as shown in Fig. 26(b), resulting in a much weaker observed limit of $m_{Z'} > 835 \text{ GeV}$ compared to an expectation of 920 GeV for narrow resonances. This excess was not confirmed by CDF, which excluded narrow Z' bosons up to an observed (expected) limit of $m_{Z'} > 915 (940) \text{ GeV}$ using 9.5 fb^{-1} of data. The sensitivity of such searches dramatically decreases beyond $m_{Z'} > 1 \text{ TeV}$ because the three jets from the $t \rightarrow W^+(q'\bar{q})b$ decay can overlap in (η, ϕ) and are not resolved as separate objects. This experimental challenge can be addressed by applying jet substructure techniques [244] to identify sub-jets resulting from the $t \rightarrow W^+(q'\bar{q})b$ decay products within wide jets. ATLAS performed a search for Z' resonances using 20.3 fb^{-1} of data, and obtained observed (expected) exclusion limits of $m_{Z'} > 1.8 (2) \text{ TeV}$ for narrow and of $2.1 (2.2) \text{ TeV}$ for wide resonances in Randall-Sundrum scenarios [245]. The search by CMS using 19.7 fb^{-1} of data found observed (expected) exclusion limits of $m_{Z'} > 2.4 (2.4) \text{ TeV}$ for narrow resonances as shown in Fig. 27, and of $2.8 (2.7) \text{ TeV}$ for wide resonances in Randall-Sundrum models [246].

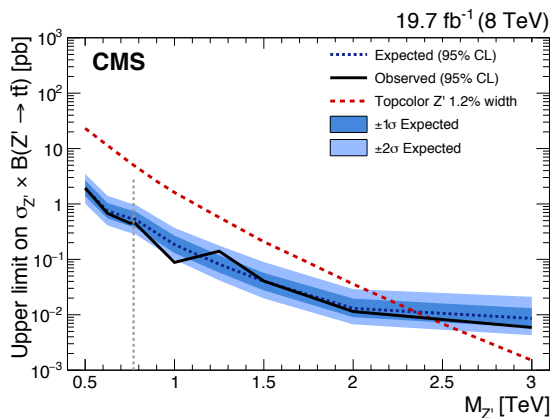


Figure 27: Observed and expected upper limits on a narrow topcolor $Z' \rightarrow t\bar{t}$ resonance as a function of $M_{Z'}$ [246]. The shaded regions around the expected limit represent the ± 1 and ± 2 standard deviation bands. The predicted $\sigma_{Z'} \times \mathcal{B}(Z' \rightarrow t\bar{t})$ is also given.

10 Conclusions

The top quark is strikingly different from other quarks and thus it plays a unique role in particle physics. It is the most massive of the quarks, and indeed of all SM particles. Because the Higgs Yukawa coupling is proportional to fermion mass, the top quark Yukawa coupling is large – very close to unity. The large mass also makes the top quark lifetime very much shorter than the time required to pull new quark-antiquark states out of the vacuum and make hadrons so, uniquely, the top quark can be studied in its bare, un-hadronized form. Despite the top quark’s similarities to the other fermions in its basic quantum properties, it stands out as the exotic bird of paradise in the quark family portrait. Or is the top the model for what a quark should be, with the others as the odd sisters?

The virtual top quark loops in the W or Higgs boson propagators lead to very sensitive tests of the validity of the SM through the relationship of the masses of the top quark, the W boson and the Higgs boson. The measured top quark mass is consistent with what is needed to drive the quartic coupling in the SM Higgs potential to negative values at large Q^2 , leading to a possibly metastable universe. While the lifetime of the universe is extremely long, it is a puzzle that the top and Higgs masses should conspire so as to put the SM at the boundary between stability and instability.

In seeking new phenomena to explain the defects of the SM, most new models invoke large couplings between the new particles and the top quark, as seen in the very large Yukawa coupling of the Higgs boson to top quarks. Thus we have the prospect of finding new particles such as heavy Z bosons or vector quarks whose decays contain top quarks, or particles such as charged Higgs bosons that could appear in the top decays. In supersymmetric models, the need for cancellation of the large loop contributions arising from the large top quark mass suggests that the companion top squarks should have a lower mass than other sparticle masses, thus making them prime candidates for a first sighting of supersymmetry. Despite the failure so far to find new physics in the production or decays of top quarks, the searches remain highly motivated and will continue to be a dominant theme in the ongoing LHC program.

Although the top quark might seem to play no role in our everyday experience, its impact is nevertheless strong. If one assumes approximately unified $SU(3) \times SU(2) \times U(1)$ couplings at a very high scale and allows them to evolve with decreasing Q^2 , a break in the running α_s occurs at $Q = m_t$. If one continues to evolve to lower Q^2 , one reaches the scale Λ_{QCD} , which in turn determines the proton mass. The resulting relation [247] $m_{\text{proton}} \propto m_t^{2/27}$ implies that if the top quark mass had the value originally expected of about $3 \times m_b$, the proton would weigh only 80% of what we observe, with dramatic consequences for our everyday world.

We expect the top quark to continue to be a portal for new discoveries.

Acknowledgements

We gratefully acknowledge support from the Federal Ministry of Education and Research (Germany); Ministry of Education and Science of the Russian Federation, National Research Center “Kurchatov Institute” of the Russian Federation, Russian Foundation for Basic Research (Russia); and Department of Energy and National Science Foundation (United States). The work of E.B. was supported in part by the Ministry of Education and Science of the Russian Federation under the grant number NS-3042.2014.2.

References

- [1] F. Abe *et al.* (CDF Collaboration), “*Observation of top quark production in $\bar{p}p$ collisions*”, Phys. Rev. Lett. **74**, 2626 (1995).
- [2] S. Abachi *et al.* (D0 Collaboration), “*Observation of the top quark*”, Phys. Rev. Lett. **74**, 2632 (1995).
- [3] M. Gell-Mann, “*A schematic model of baryons and mesons*”, Phys. Lett. **8**, 214 (1964).
- [4] G. Zweig, “*An $SU(3)$ model for strong interaction symmetry and its breaking*”, 2, CERN-TH-412 (1964).
- [5] J. Aubert, *et al.*, “*Experimental observation of a heavy particle J* ”, Phys. Rev. Lett. **33**, 1404 (1974).
- [6] J. Augustin, *et al.*, “*Discovery of a narrow resonance in e^+e^- annihilation*”, Phys. Rev. Lett. **33**, 1406 (1974).
- [7] S. L. Glashow, J. Iliopoulos, L. Maiani, “*Weak interactions with lepton-hadron symmetry*”, Phys. Rev. D **2**, 1285 (1970).
- [8] M. L. Perl, *et al.*, “*Evidence for anomalous lepton production in e^+e^- annihilation*”, Phys. Rev. Lett. **35**, 1489 (1975).
- [9] S. W. Herb *et al.*, “*Observation of a dimuon resonance at 9.5 GeV in 400 GeV proton-nucleus collisions*”, Phys. Rev. Lett. **39**, 252 (1977).
- [10] ATLAS, CDF, CMS and D0 Collaborations, “*First combination of Tevatron and LHC measurements of the top-quark mass*”, [arXiv:1403.4427 \[hep-ex\]](https://arxiv.org/abs/1403.4427) (2014).

- [11] N. Cabibbo, “*Unitary symmetry and leptonic decays*”, Phys. Rev. Lett. **10**, 531 (1963).
- [12] M. Kobayashi and T. Maskawa, “*CP-violation in the renormalizable theory of weak interaction*”, Prog. Theor. Phys. **49**, 652 (1973).
- [13] M. Jezabek and J. H. Kuhn, “*The top width: theoretical update*”, Phys. Rev. D **48**, 1910 (1993), erratum-ibid. D **49**, 4970 (1994).
- [14] M. Jezabek and J. H. Kuhn, “*QCD corrections to semileptonic decays of heavy quarks*”, Nucl. Phys. B **314**, 1 (1989).
- [15] I. I. Bigi, Y. L. Dokshitzer, V. A. Khoze, J. H. Kuhn and P. M. Zerwas, “*Production and decay properties of ultraheavy quarks*”, Phys. Lett. B **181**, 157 (1986).
- [16] D. Abbaneo *et al.* (LEP Electroweak Working Group and SLD Heavy Flavor Group Collaborations), “*A Combination of preliminary electroweak measurements and constraints on the Standard Model*”, CERN-PPE-96-183, SLAC-REPRINT-1996-037.
- [17] M. Baak, J. Cuth, J. Haller, A. Hoecker, R. Kogler, K. Moenig, M. Schott, and J. Stelzer, “*The global electroweak fit at NNLO and prospects for the LHC and ILC*”, Eur. Phys. J. C **74**, 3046 (2014).
- [18] V. Branchina, E. Messina, A. Platania, “*Top mass determination, Higgs inflation, and vacuum stability*”, J. High Energy Phys. **1409**, 182 (2014).
- [19] S. Weinberg “*A Model of Leptons*”, Phys. Rev. Lett. **19**, 1264 (1967).
- [20] A. Salam *Elementary Particle Physics: Relativistic Groups and Analyticity* (8th Nobel Symposium), Almquist and Wiksell International, ed. N. Svartholm, Stockholm 1968, p. 367.
- [21] S. L. Glashow, Nucl. Phys. **22**, 579 (1961).
- [22] B. Adeva *et al.* (MARK-J Collaboration), “*Search for top quark and a test of models without top quark at the highest PETRA energies*”, Phys. Rev. Lett. **50**, 799 (1983).
- [23] H. J. Behrend *et al.* (CELLO Collaboration), “*Search for new heavy quarks in e^+e^- collisions up to 46.78 GeV center-of-mass energy*”, Phys. Lett. B **144**, 297 (1984).

- [24] M. Altho *et al.* (TASSO Collaboration), “*Measurement of R and search for top quark in e^+e^- annihilation between 39.8 GeV and 45.2 GeV*”, Phys. Lett. B **138**, 441 (1984).
- [25] K. Abe *et al.* (VENUS Collaboration), “*Measurement of R and search for new quark flavors decaying into multi-jet final states in e^+e^- collisions between 54 GeV and 61.4 GeV c.m. energies*”, Phys. Lett. B **234**, 382 (1990).
- [26] G. S. Abrams *et al.* (MARK II Collaboration), “*Searches for new quarks and leptons produced in Z boson decay*”, Phys. Rev. Lett. **63**, 2447 (1989).
- [27] D. Decamp *et al.* (ALEPH Collaboration), “*A search for new quarks and leptons from Z^0 decay*”, Phys. Lett. B **236**, 511 (1990).
- [28] P. Abreu *et al.* (DELPHI Collaboration), “*Search for t and b' quarks in hadronic decays of the Z^0 boson*”, Phys. Lett. B **242**, 536 (1990).
- [29] M. Z. Akrawy *et al.* (OPAL Collaboration), “*A Search for the top and b' quarks in hadronic Z^0 Decays*”, Phys. Lett. B **236**, 364 (1990).
- [30] G. Arnison *et al.* (UA1 Collaboration), “*Associated production of an isolated, large-transverse-momentum lepton (electron or muon), and two jets at the CERN $p\bar{p}$ collider*”, Phys. Lett. B **147**, 493 (1984).
- [31] C. Albajar *et al.* (UA1 Collaboration), “*Search for new heavy quarks at the CERN proton-antiproton collider*”, Z. Phys. C **37**, 505 (1988).
- [32] T. Akesson *et al.* (UA2 Collaboration), “*Search for top quark production at the CERN $p\bar{p}$ collider*”, Z. Phys. C **46**, 179 (1990).
- [33] F. Abe *et al.* (CDF Collaboration), “*Lower limit on the top quark mass from events with two leptons in $p\bar{p}$ collisions at $\sqrt{s} = 1.8$ TeV*”, Phys. Rev. Lett. **68**, 447 (1992).
- [34] S. D. Holmes and V. Shiltsev, “*The legacy of the Tevatron in the area of accelerator science*”, Annu. Rev. Nucl. Part. Sci, **63**, 435 (2013).
- [35] S. Abachi *et al.* (D0 Collaboration), “*Search for High Mass Top Quark Production in $p\bar{p}$ Collisions at $\sqrt{s} = 1.8$ TeV*”, Phys. Rev. Lett. **72**, 2138 (1994).
- [36] F. Abe *et al.* (CDF Collaboration), “*Evidence for top quark production in $p\bar{p}$ collisions at $\sqrt{s} = 1.8$ TeV*”, Phys. Rev. D **50**, 2996 (1994).

- [37] P. D. Grannis, “*Search for the top quark: results from the D0 experiment*”, Proceedings of the XXVII International Conference on High Energy Physics, p. 15, Institute of Physics Publishing, Glasgow UK (1994). See also S. Abachi *et al.* (D0 Collaboration), “*Top quark search with the D0 1992 - 1993 data sample*”, Phys. Rev. D **52**, 4877 (1995) for a slightly updated version of this analysis.
- [38] M. Czakon, P. Fiedler, A. Mitov, “*Total top-quark pair-production cross section at hadron colliders through $O(\alpha_s^4)$* ”, Phys. Rev. Lett. **110**, 252004 (2013).
- [39] M. Czakon, P. Fiedler, A. Mitov, “*Resolving the Tevatron top quark forward-backward asymmetry puzzle: fully differential next-to-next-to-leading-order calculation*” Phys. Rev. Lett. **115**, 052001 (2015).
- [40] T. Aaltonen *et al.* (CDF and D0 Collaborations), “*Combination of measurements of the top-quark pair production cross section from the Tevatron collider*”, Phys. Rev. D **89**, 072001 (2014).
- [41] V. Abazov *et al.* (D0 Collaboration), “*Measurement of the inclusive $t\bar{t}$ production cross section in $p\bar{p}$ collisions at $\sqrt{s} = 1.96$ TeV*”, D0 Note 6453-CONF (2015), to be submitted for publication in Phys. Rev. D.
- [42] ATLAS and CMS Collaborations, “*Combination of ATLAS and CMS top quark pair cross section measurements in the $e\mu$ final state using proton-proton collisions at 8 TeV*”, ATLAS-CONF-2014-054 and CMS-PAS-TOP-14-016 (2014).
- [43] R. Aaij *et al.* (LHCb Collaboration), “*First observation of top quark production in the forward region*”, Phys. Rev. Lett. **115**, 112001 (2015).
- [44] V. Abazov *et al.* (D0 Collaboration), “*Measurement of differential $t\bar{t}$ production cross sections in $p\bar{p}$ collisions*”, Phys. Rev. D **90**, 092006 (2014).
- [45] G. Aad *et al.* (ATLAS Collaboration), “*Differential top-antitop cross-section measurements as a function of observables constructed from final-state particles using pp collisions at $\sqrt{s} = 7$ TeV in the ATLAS detector*”, J. of High Energy Phys. **1506**, 100 (2015).
- [46] R. Röntsch and M. Schulze, “*Constraining couplings of the top quarks to the Z boson in $t\bar{t} + Z$ production at the LHC*”, J. of High Energy Phys. **1407**, 91 (2014).
- [47] G. Aad *et al.* (ATLAS Collaboration), “*Study of heavy-flavor quarks produced in association with top-quark pairs at $\sqrt{s} = 7$ TeV using the ATLAS detector*”, Phys. Rev. D **89**, 072012 (2014).

- [48] G. Aad *et al.* (ATLAS Collaboration), “Search for $t\bar{t}Z$ production in the three lepton final state with 4.7 fb^{-1} of $\sqrt{s} = 7 \text{ TeV}$ pp collision data collected by the ATLAS detector”, ATLAS-CONF-2012-126 (2012).
- [49] S. Chatrchyan *et al.* (CMS Collaboration), “Measurement of associated production of vector bosons and top quark-antiquark pairs in pp collisions at $\sqrt{s} = 7 \text{ TeV}$ ”, Phys. Rev. Lett. **110** 172002 (2013).
- [50] G. Aad *et al.* (ATLAS Collaboration), “Evidence for the associated production of a vector boson (W, Z) and top quark pair in the dilepton and trilepton channels in pp collision data at $\sqrt{s} = 8 \text{ TeV}$ collected by the ATLAS detector at the LHC”, ATLAS-CONF-2014-038 (2014).
- [51] S. Chatrchyan *et al.* (CMS Collaboration), “Measurement of top quark-antiquark pair production in association with a W or Z boson in pp collisions at $\sqrt{s} = 8 \text{ TeV}$ ”, Eur. Phys. J. C **74** 3060 (2014).
- [52] S. Chatrchyan *et al.* (CMS Collaboration), “Measurement of the cross section ratio $\sigma(t\bar{t}b\bar{b})/\sigma(t\bar{t}jj)$ in pp collisions at $\sqrt{s} = 8 \text{ TeV}$ ”, Phys. Lett. B **746**, 132 (2015).
- [53] G. Aad *et al.* (ATLAS Collaboration), “Search for exotic same-sign dilepton signatures (b' quark, $T_{5/3}$ and four top quarks production) in 4.7 fb^{-1} of pp collisions at $\sqrt{s} = 7 \text{ TeV}$ with the ATLAS detector”, ATLAS-CONF-2012-130 (2012).
- [54] G. Aad *et al.* (ATLAS Collaboration), “Search for anomalous production of events with same-sign dileptons and b jets in 14.3 fb^{-1} of pp collisions at $\sqrt{s} = 8 \text{ TeV}$ with the ATLAS detector”, ATLAS-CONF-2013-051 (2013).
- [55] S. Chatrchyan *et al.* (CMS Collaboration), “Search for Standard Model production of four top quarks in the lepton + jets channel in pp collisions at $\sqrt{s} = 8 \text{ TeV}$ ”, J. High Energy Phys. **1411**, 154 (2014).
- [56] T. Aaltonen *et al.* (CDF Collaboration), “Evidence for a mass dependent forward-backward asymmetry in top quark pair production”, Phys. Rev. D **83**, 112003 (2011).
- [57] V. Abazov *et al.* (D0 Collaboration), “Forward-backward asymmetry in top quark-antiquark production”, Phys. Rev. D **84**, 112005 (2011).
- [58] J.A. Aguilar-Saavedra, D. Amidei, A. Juste, M. Pérez-Victoria, “Asymmetries in top quark pair production at hadron colliders”, Rev. Mod. Phys. **87**, 421 (2015).

- [59] T. Aaltonen *et al.* (CDF Collaboration), “*Measurement of the top quark forward-backward production asymmetry and its dependence on event kinematic properties*”, Phys. Rev. D **87**, 092002 (2013).
- [60] V. Abazov *et al.* (D0 Collaboration), “*Measurement of the forward-backward asymmetry in top quark-antiquark production in $p\bar{p}$ collisions using the lepton+jets channel*”, Phys. Rev. D **90**, 072011 (2014).
- [61] V. Abazov *et al.* (D0 Collaboration), “*Simultaneous measurement of forward-backward asymmetry and top polarization in dilepton final states from $t\bar{t}$ production at the Tevatron*”, Phys. Rev. D **92**, 052007 (2015).
- [62] T. Aaltonen *et al.* (CDF Collaboration), “*Measurement of the inclusive leptonic asymmetry in top-quark pairs that decay to two charged leptons at CDF*”, Phys. Rev. Lett. **113**, 042001 (2014).
- [63] V. Abazov *et al.* (D0 Collaboration), “*Measurement of the forward-backward asymmetry in the distribution of leptons in $t\bar{t}$ events in the lepton+jets channel*”, Phys. Rev. D **90**, 072001 (2014).
- [64] W. Bernreuther and Z.-G. Si, “*Top quark and leptonic charge asymmetries for the Tevatron and LHC*”, Phys. Rev. D **86**, 034026 (2012).
- [65] V. Abazov *et al.* (D0 Collaboration), “*Measurement of the asymmetry in angular distributions of leptons produced in dilepton $t\bar{t}$ final states in $p\bar{p}$ collisions at $\sqrt{s} = 1.96\text{ TeV}$* ”, Phys. Rev. D **88**, 112002 (2013).
- [66] G. Aad *et al.* (ATLAS Collaboration), “*Measurement of the top quark pair production charge asymmetry in proton-proton collisions at 7 TeV using the ATLAS detector*”, J. High Energy Phys. **1402**, 107 (2014).
- [67] G. Aad *et al.* (ATLAS Collaboration), “*Measurement of the charge asymmetry in dileptonic decays of top quark pairs in pp collisions at $\sqrt{s} = 7\text{ TeV}$ using the ATLAS detector*”, J. of High Energy Phys. **1505**, 61 (2015).
- [68] S. Chatrchyan *et al.* (CMS Collaboration), “*Inclusive and differential measurements of the charge asymmetry in proton-proton collisions at $\sqrt{s} = 7\text{ TeV}$* ”, Phys. Lett. B **717**, 129 (2012).
- [69] S. Chatrchyan *et al.* (CMS Collaboration), “*Inclusive and differential measurements of the $t\bar{t}$ charge asymmetry in pp collisions at $\sqrt{s} = 8\text{ TeV}$* ”, CMS-PAS-TOP-12-033.

- [70] S. Chatrchyan *et al.* (CMS Collaboration), “*Measurements of the $t\bar{t}$ charge asymmetry using the dilepton decay channel in pp collisions at $\sqrt{s} = 7$ TeV*”, J. High Energy Phys. **1404**, 191 (2014).
- [71] V. Abazov *et al.* (D0 Collaboration), “*Evidence for spin correlation in $t\bar{t}$ production*”, Phys. Rev. Lett. **108**, 032004 (2012).
- [72] W. Bernreuther, A. Brandenburg, Z.G. Si, and P. Uwer, “*Top quark pair production and decay at hadron colliders*”, Nucl. Phys B **690**, 81 (2004).
- [73] T. Aaltonen *et al.* (CDF Collaboration), “*Measurement of $t\bar{t}$ spin correlation in $p\bar{p}$ collisions using the CDF II detector at the Tevatron*”, Phys. Rev. D **83**, 031104 (2011).
- [74] G. Aad *et al.* (ATLAS Collaboration), “*Observation of spin correlation in $t\bar{t}$ events from pp collisions at $\sqrt{s} = 7$ TeV using the ATLAS detector*”, Phys. Rev. Lett. **108**, 212001 (2012).
- [75] S. Chatrchyan *et al.* (CMS Collaboration), “*Measurements of $t\bar{t}$ spin correlations and top-quark polarization using dilepton final states in pp Collisions at $\sqrt{s} = 7$ TeV*”, Phys. Rev. Lett. **112**, 182001 (2014).
- [76] G. Aad *et al.* (ATLAS Collaboration), “*Measurements of spin correlation in top-antitop quark events from proton-proton collisions at $\sqrt{s} = 7$ TeV using the ATLAS detector*”, Phys. Rev. D **90**, 112016 (2014).
- [77] D0 Collaboration, “*Measurement of top quark polarization in the lepton + jet final state*”, D0 Note 6471-CONF (2015).
- [78] G. Aad *et al.* (ATLAS Collaboration), “*Measurement of top quark polarization in top-antitop events from proton-proton collisions at $\sqrt{s} = 7$ TeV using the ATLAS Detector*”, Phys. Rev. Lett. **111**, 232002 (2014).
- [79] S. Chatrchyan *et al.* (CMS Collaboration), “*Measurement of top quark polarization in t -channel single-top production*”, CMS-PAS-TOP-13-001 (2014).
- [80] S. S. D. Willenbrock and D. A. Dicus, “*Production of heavy quarks from W -gluon fusion*”, Phys. Rev. D **34**, 155 (1986).
- [81] N. Kidonakis, “*Single top quark production at the Fermilab Tevatron: threshold resummation and finite-order soft gluon corrections*”, Phys. Rev. D **74**, 114012 (2006).
- [82] T. Aaltonen *et al.* (CDF Collaboration), “*Observation of electroweak single top-quark production*”, Phys. Rev. Lett. **103**, 092002 (2009).

- [83] V. Abazov, *et al.* (D0 Collaboration), “*Observation of single top-quark production*”, Phys. Rev. Lett. **103**, 092001 (2009).
- [84] L. Breiman *et al.*, *Classification and regression trees* (Wadsworth, Stamford, 1984).
- [85] R. M. Neal, *Bayesian learning for neural networks* (Springer-Verlag, New York, 1996).
- [86] E. E. Boos *et al.*, “*Method for simulating electroweak top-quark production events in the NLO approximation: SingleTop event generator*”, Phys. Atom. Nucl. **69**, 1317 (2006).
- [87] T. A. Aaltonen *et al.* (CDF and D0 Collaborations), “*Observation of s-channel production of single top quarks at the Tevatron*”, Phys. Rev. Lett. **112**, 231803 (2014).
- [88] T. A. Aaltonen *et al.* (CDF and D0 Collaborations), “*Tevatron combination of single-top-quark cross sections and determination of the magnitude of the Cabibbo-Kobayashi-Maskawa matrix element V_{tb}* ”, Phys. Rev. Lett. **115**, 152003 (2015).
- [89] N. Kidonakis, “*Differential and total cross sections for top pair and single top production*”, Proceedings of the XX International Workshop on Deep-Inelastic Scattering and Related Subjects. Bonn, Germany, 2012.
- [90] N. Kidonakis, “*NNLL resummation for s-channel single top quark production*”, Phys. Rev. D **81**, 054028 (2010).
- [91] N. Kidonakis, “*NNLL threshold resummation for top-pair and single-top production*”, Phys. Part. Nucl. **45**, 714 (2014).
- [92] S. Chatrchyan *et al.* (CMS Collaboration), “*Observation of the associated production of a single top quark and a W boson in pp collisions at $\sqrt{s} = 8$ TeV*”, Phys. Rev. Lett. **112**, 231802 (2014).
- [93] J. Neyman and E. S. Pearson, “*On the problem of the most efficient tests of statistical hypotheses*”, Phil. Trans. R. Soc. Lond. A **231**, 289 (1933).
- [94] G. Aad *et al.* (ATLAS Collaboration), “*Measurement of the top quark mass in the $t\bar{t} \rightarrow \text{lepton} + \text{jets}$ and $t\bar{t} \rightarrow \text{dilepton}$ channels using $\sqrt{s} = 7$ TeV ATLAS data*”, Eur. Phys. J. C **75**, 330 (2015).

- [95] G. Aad *et al.* (ATLAS Collaboration), “*Measurement of the top quark mass in topologies enhanced with single top quarks produced in the t -channel at $\sqrt{s} = 8$ TeV using the ATLAS experiment*”, ATLAS-CONF-2014-055 (2014).
- [96] G. Aad *et al.* (ATLAS Collaboration), “*Measurement of the top-quark mass in the fully hadronic decay channel from ATLAS data at $\sqrt{s} = 7$ TeV*”, Eur. Phys. J. C, **75**, 158 (2015).
- [97] T. Aaltonen *et al.* (CDF Collaboration), “*Top quark mass measurement in the dilepton channel using the full CDF data set*”, CDF Note 11072 (2014).
- [98] T. Aaltonen *et al.* (CDF Collaboration), “*Precision top-quark mass measurements at CDF*”, Phys. Rev. Lett. **109**, 152003 (2012).
- [99] T. Aaltonen *et al.* (CDF Collaboration), “*Measurement of the top quark mass with in situ jet energy scale calibration in the all-hadronic channel using the template method with 9.3 fb $^{-1}$* ”, CDF Note 11084 (2014).
- [100] T. Aaltonen *et al.* (CDF Collaboration), “*Top-quark mass measurement in events with jets and missing transverse energy using the full CDF data set*”, Phys. Rev. D **88**, 011101 (2013).
- [101] S. Chatrchyan *et al.* (CMS Collaboration), “*Measurement of the top quark mass in dilepton $t\bar{t}$ decays at $\sqrt{s} = 8$ TeV*”, CMS-PAS-TOP-14-014 (2014).
- [102] S. Chatrchyan *et al.* (CMS Collaboration), “*Measurement of the top-quark mass in $t\bar{t}$ events with lepton+jets final states in pp collisions at $\sqrt{s} = 8$ TeV*”, CMS-PAS-TOP-14-001 (2014).
- [103] S. Chatrchyan *et al.* (CMS Collaboration), “*Measurement of the top-quark mass in $t\bar{t}$ events with all-jets final states in pp collisions at $\sqrt{s} = 8$ TeV*”, CMS-PAS-TOP-14-002 (2014).
- [104] V. M. Abazov *et al.* (D0 Collaboration), “*Precise measurement of the top quark mass in dilepton decays using optimized neutrino weighting*”, Phys. Lett. B **752**, 18 (2015).
- [105] V. M. Abazov *et al.* (D0 Collaboration), “*Precision measurement of the top quark mass in lepton+jets final states at D0*”, Phys. Rev. Lett. **113**, 032002 (2014).
- [106] W. Bernreuther, private communication (2012).
- [107] K. Olive *et al.* (Particle Data Group), “*Review of Particle Physics*”, Chin. Phys. C **38**, 090001 (2014).

- [108] V. M. Abazov *et al.* (D0 Collaboration), “Precision measurement of the top quark mass in lepton+jets final states at $D0$ ”, Phys. Rev. D **91**, 112003 (2015).
- [109] O. Brandt, G. Gutierrez, M.H.L.S. Wang, and Z. Ye, “Acceleration of matrix element computations for precision measurements”, Nucl. Instrum. Meth. A, **775**, 27 (2015).
- [110] V. M. Abazov *et al.* (D0 Collaboration), “Precise measurement of the top-quark mass from lepton+jets events at $D0$ ”, Phys. Rev. D **84**, 032004 (2011).
- [111] L. Lyons, D. Gibaut, and P. Clifford, “How to combine correlated estimates of a single physical quantity”, Nucl. Instrum. Meth. A **270**, 110 (1988).
- [112] A. Valassi, “Combining correlated measurements of several different physical quantities”, Nucl. Instrum. Meth. A **500**, 391 (2003).
- [113] T. Aaltonen *et al.* (CDF and D0 Collaborations), “Combination of CDF and D0 results on the mass of the top quark using up to 9.7 fb^{-1} at the Tevatron”, [arXiv:1407.2682 \[hep-ex\]](https://arxiv.org/abs/1407.2682) (2014).
- [114] I. I. Bigi, M. A. Shifman, N. G. Uraltsev, A. I. Vainshtein, “Pole mass of the heavy quark: perturbation theory and beyond”, Phys. Rev. D **50**, 2234 (1994).
- [115] M. Beneke and V. M. Braun, “Heavy quark effective theory beyond perturbation theory: renormalons, the pole mass and the residual mass term”, Nucl. Phys. B **426**, 301 (1994).
- [116] M. C. Smith and S. S. Willenbrock, “Top-quark pole mass”, Phys. Rev. Lett. **79**, 3825 (1997).
- [117] W. A. Bardeen, A. J. Buras, D. W. Duke, and T. Muta, “Deep-inelastic scattering beyond the leading order in asymptotically free gauge theories”, Phys. Rev. D **18**, 3998 (1978).
- [118] S. Fleming, A. H. Hoang, S. Mantry, and I. W. Stewart, “Factorization approach for top mass reconstruction at high energies”, eConf **C0705302**, “LOOP06” (2007).
- [119] A. H. Hoang and I. W. Stewart, “Top mass measurements from jets and the Tevatron top-quark mass”, Nucl. Phys. Proc. Suppl. **185**, 220 (2008).
- [120] A. Buckley *et al.*, “General-purpose event generators for LHC physics”, Phys. Rept. **504**, 145 (2011).

- [121] T. Aaltonen *et al.* (CDF Collaboration), “*Cross section constrained top quark mass measurement from dilepton events at the Tevatron*”, Phys. Rev. Lett. **100**, 062005 (2008).
- [122] V. M. Abazov *et al.* (D0 Collaboration), “*Measurement of the $t\bar{t}$ production cross section in $p\bar{p}$ collisions at $\sqrt{s} = 1.96$ -TeV*”, Phys. Rev. Lett. **100**, 192004 (2008).
- [123] M. Cacciari, S. Frixione, M.L. Mangano, P. Nason, and G. Ridolfi, “*The $t\bar{t}$ cross-section at 1.8 and 1.96 TeV: a study of the systematics due to parton densities and scale dependence*”, J. High Energy Phys. **0404**, 068 (2004).
- [124] G. Aad *et al.* (ATLAS Collaboration), “*Measurement of the $t\bar{t}$ production cross-section using $e\mu$ events with b -tagged jets in pp collisions at $\sqrt{s} = 7$ and 8 TeV with the ATLAS detector*”, Eur. Phys. J. C **74**, 3109 (2014).
- [125] S. Chatrchyan *et al.* (CMS Collaboration), “*Determination of the top-quark pole mass and strong coupling constant from the $t\bar{t}$ production cross section in pp collisions at $\sqrt{s} = 7$ TeV*”, Phys. Lett. B **728**, 496 (2014).
- [126] S. Alioli, P. Fernandez, J. Fuster, A. Irlles, S.-O. Moch, P. Uwer, and M. Vos, “*A new observable to measure the top-quark mass at hadron colliders*”, Eur. Phys. J. C **73**, 2438 (2013).
- [127] G. Aad *et al.* (ATLAS Collaboration), “*Determination of the top-quark pole mass using $t\bar{t} + 1$ jet events collected with the ATLAS experiment in 7 TeV pp collisions*”, ATLAS-CONF-2014-053 (2014).
- [128] J. Gao J, C. S. Li, and H. X. Zhu, “*Top-quark decay at next-to-next-to-leading order in QCD*”, Phys. Rev. Lett. **110**, 042001 (2013).
- [129] T. Aaltonen *et al.* (CDF Collaboration), “*First direct limit on the top quark lifetime*”, CDF Note 8104, (2005).
- [130] T. Aaltonen *et al.* (CDF Collaboration), “*Direct measurement of the total decay width of the top quark*”, Phys. Rev. Lett. **111**, 202001 (2013).
- [131] V. M. Abazov *et al.* (D0 Collaboration), “*Improved determination of the width of the top quark*”, Phys. Rev. D **85**, 091104 (2012).
- [132] V. M. Abazov *et al.* (D0 Collaboration), “*Model-independent measurement of t -channel single top quark production in $p\bar{p}$ collisions at $\sqrt{s} = 1.96$ TeV*”, Phys. Lett. B **705**, 313 (2011).

- [133] V. M. Abazov *et al.* (D0 Collaboration), “Precision measurement of the ratio $B(t \rightarrow Wb)/B(t \rightarrow Wq)$ and extraction of V_{tb} ”, Phys. Rev. Lett. **107**, 121802 (2011).
- [134] S. Chatrchyan *et al.* (CMS Collaboration), “Measurement of the ratio $B(t \rightarrow Wb)/B(t \rightarrow Wq)$ in pp collisions at $\sqrt{s} = 8$ TeV”, Phys. Lett. B **736**, 33 (2014).
- [135] S. Chatrchyan *et al.* (CMS Collaboration), “Measurement of the single-top-quark t -channel cross section in pp collisions at $\sqrt{s} = 7$ TeV”, J. High Energy Phys. **1212**, 035 (2012).
- [136] N. Kidonakis, “Next-to-next-to-leading-order collinear and soft gluon corrections for t -channel single top quark production”, Phys. Rev. D **83**, 091503 (2011).
- [137] D. Colladay and V. A. Kostelecky, “CPT violation and the Standard Model”, Phys. Rev. D **55**, 6760 (1997).
- [138] O. W. Greenberg, “CPT violation implies violation of Lorentz invariance”, Phys. Rev. Lett. **89**, 231602 (2002).
- [139] G. Barenboim and J. Lykken, “A model of CPT violation for neutrinos”, Phys. Lett. B **554**, 73 (2003).
- [140] V. M. Abazov *et al.* (D0 Collaboration), “Direct measurement of the mass difference between top and antitop quarks”, Phys. Rev. D **84**, 052005 (2011).
- [141] T. Aaltonen *et al.* (CDF Collaboration), “Measurement of the mass difference between top and antitop quarks”, Phys. Rev. D **87**, 052013 (2013).
- [142] S. Chatrchyan *et al.* (CMS Collaboration), “Measurement of the mass difference between top and antitop quarks”, J. High Energy Phys. **1206**, 109 (2012).
- [143] G. Aad *et al.* (ATLAS Collaboration), “Measurement of the mass difference between top and antitop quarks in pp collisions at $\sqrt{s} = 7$ TeV using the ATLAS detector”, Phys. Lett. B **728**, 363 (2014).
- [144] D. Chang, W. Chang and E. Ma, “Alternative interpretation of the Fermilab Tevatron top events”, Phys. Rev. D **59**, 091503 (1999).
- [145] D. Chang, W. Chang, and E. Ma, “Fitting precision electroweak data with exotic heavy quarks”, Phys. Rev. D **61**, 037301 (2000).

- [146] V. M. Abazov *et al.* (D0 Collaboration), “*Experimental discrimination between charge $2e/3$ top quark and charge $4e/3$ exotic quark production scenarios*”, Phys. Rev. Lett. **98**, 041801 (2007).
- [147] V. M. Abazov *et al.* (D0 Collaboration), “*Measurement of the electric charge of the top quark in $t\bar{t}$ events*”, Phys. Rev. D **90**, 051101 (2014).
- [148] T. Aaltonen *et al.* (CDF Collaboration), “*Exclusion of exotic top-like quarks with $-4/3$ electric charge using jet-charge tagging in single-lepton $t\bar{t}$ events at CDF*”, Phys. Rev. D **88**, 032003 (2013).
- [149] G. Aad *et al.* (ATLAS Collaboration), “*Measurement of the top quark charge in pp collisions at $\sqrt{s} = 7$ TeV with the ATLAS detector*”, J. High Energy Phys. **1311**, 031 (2013).
- [150] T. Aaltonen *et al.* (CDF Collaboration), “*Observation of single top quark production and measurement of $|V_{tb}|$ with CDF*”, Phys. Rev. D **82**, 112005 (2010).
- [151] V. M. Abazov *et al.* (D0 Collaboration), “*Measurements of single top quark production cross sections and $|V_{tb}|$ in $p\bar{p}$ collisions at $\sqrt{s} = 1.96$ TeV*”, Phys. Rev. D **84**, 112001 (2011).
- [152] G. L. Kane, G. A. Ladinsky, and C. P. Yuan, “*Using the top quark for testing standard-model polarization and CP predictions*”, Phys. Rev. D **45**, 124 (1992).
- [153] A. Czarnecki, J. G. Korner and J. H. Piclum, “*Helicity fractions of W bosons from top quark decays at next-to-next-to-leading order in QCD*”, Phys. Rev. D **81**, 111503 (2010).
- [154] T. Aaltonen *et al.* (CDF and D0 Collaborations), “*Combination of CDF and D0 measurements of the W boson helicity in top quark decays*”, Phys. Rev. D **85**, 071106 (2012).
- [155] T. Aaltonen *et al.* (CDF Collaboration), “*Measurement of W -boson polarization in top-quark decay using the full CDF Run II data set*”, Phys. Rev. D **87**, 031104(R) (2013).
- [156] G. Aad *et al.* (ATLAS Collaboration), “*Measurement of the W boson polarization in top quark decays with the ATLAS detector*”, J. High Energy Phys. **1206**, 088 (2012).

- [157] S. Chatrchyan *et al.* (CMS Collaboration), “*Measurement of the W boson helicity in events with a single reconstructed top quark in pp collisions at $\sqrt{s} = 8$ TeV*”, J. High Energy Phys. **1501**, 053 (2015).
Phys. Rev. Lett. **10**, 531 (1961).
- [158] D. Atwood, S. K. Gupta, A. Soni, “*Detecting fourth generation quarks at hadron colliders*”, J. High Energy Phys. **1206**, 205 (2012).
- [159] T. Aaltonen *et al.* (CDF Collaboration), “*Measurement of $R = B(t \rightarrow Wb)/B(t \rightarrow Wq)$ in top-quark-pair decays using lepton+jets events and the full CDF Run II dataset*”, Phys. Rev. D **87**, 111101(R) (2013).
- [160] T. Aaltonen *et al.* (CDF Collaboration), “*Measurement of $B(t \rightarrow Wb)/B(t \rightarrow Wq)$ in top-quark-pair decays using dilepton events and the full CDF Run II data set*”, Phys. Rev. Lett. **112**, 221801 (2014).
- [161] P. W. Higgs, “*Broken symmetries, massless particles and gauge fields*”, Phys. Rev. Lett. **12**, 132 (1964).
- [162] P. W. Higgs, “*Broken symmetries and the masses of gauge bosons*”, Phys. Rev. Lett. **13**, 508 (1964).
- [163] P. W. Higgs, “*Spontaneous symmetry breakdown without massless bosons*”, Phys. Rev. **145**, 1156 (1966).
- [164] F. Englert and R. Brout, “*Broken symmetry and the mass of gauge vector mesons*”, Phys. Rev. Lett. **13**, 321 (1964).
- [165] G. S. Guralnik, C. R. Hagen and T. W. B. Kibble, “*Global conservation laws and massless particles*”, Phys. Rev. Lett. **13**, 585 (1964).
- [166] L.D. Faddeev and A.A. Slavnov, *Gauge fields, introduction to quantum theory*, (Addison-Wesley Publishing Company, Redwood, CA, 1991). Translation of: *Vvedenie v kvantovuiu teoriyu kalibrovochnykh polei*, A.A. Slavnov, L.D. Faddeev, Izd.3, (Moscow, 1988).
- [167] M.E. Peskin and D.V. Schroeder, *An introduction to quantum field theory* (Addison-Wesley, Reading, MA, 1995).
- [168] S. Weinberg, *The quantum theory of fields*, Vols. I, II, (Cambridge Univ. Press, Cambridge, MA, 1996).
- [169] C. Bobeth, M. Gorbahn, T. Hermann, M. Misiak, E. Stamou and M. Steinhauser, “ *$B_{s,d} \rightarrow \ell^+ \ell^-$ in the Standard Model with reduced theoretical uncertainty*”, Phys. Rev. Lett. **112**, 101801 (2014).

- [170] R. Aaij *et al.* (LHCb Collaboration), “*Measurement of the $B_s^0 \rightarrow \mu^+\mu^-$ branching fraction and search for $B^0 \rightarrow \mu^+\mu^-$ decays at the LHCb experiment*”, Phys. Rev. Lett. **111**, 101805 (2013).
- [171] S. Chatrchyan *et al.* (CMS Collaboration), “*Measurement of the B_s^0 to $\mu^+\mu^-$ branching fraction and search for B^0 to $\mu^+\mu^-$ with the CMS Experiment*”, Phys. Rev. Lett. **111**, 101804 (2013).
- [172] F. Bezrukov, A. Magnin and M. Shaposhnikov, “*Standard Model Higgs boson mass from inflation*”, Phys. Lett. B **675**, 88 (2009).
- [173] F. Bezrukov, M. Kalmykov, B. Kniehl and M. Shaposhnikov, “*Higgs boson mass and new physics*”, J. High Energy Phys. **1210**, 140 (2012).
- [174] G. Degrassi, S. Di Vita, J. Elias-Miro, J. R. Espinosa, G. F. Giudice, G. Isidori and A. Strumia, “*Higgs mass and vacuum stability in the Standard Model at NNLO*”, J. High Energy Phys. **1208**, 098 (2012).
- [175] D. Buttazzo, G. Degrassi, P. P. Giardino, G. F. Giudice, F. Sala, A. Salvio, A. Strumia, “*Investigating the near-criticality of the Higgs boson*”, J. High Energy Phys. **1312**, 089 (2013).
- [176] F. Bezrukov and M. Shaposhnikov, “*Why should we care about the top quark Yukawa coupling?*”, J. Exp. Theor. Phys. **120**, 335 (2015).
- [177] F. Bezrukov and M. Shaposhnikov, “*The Standard Model Higgs boson as the inflaton*”, Phys. Lett. B **659**, 703 (2008).
- [178] F. Bezrukov, J. Rubio and M. Shaposhnikov, “*Living beyond the edge: Higgs inflation and vacuum metastability*”, Phys. Rev. D **92**, 083512 (2015).
- [179] V. Branchina, E. Messina and A. Platania, “*Top mass determination, Higgs inflation, and vacuum stability*”, J. High Energy Phys. **1409**, 182 (2014).
- [180] E. Witten, “*Dynamical breaking of supersymmetry*”, Nucl. Phys. B **188**, 513 (1981).
- [181] E. Witten, “*Constraints on supersymmetry breaking*,” Nucl. Phys. B **202**, 253 (1982).
- [182] N. Sakai, “*Naturalness in supersymmetric GUTs*,” Z. Phys. C **11**, 153 (1981).
- [183] S. Dimopoulos and H. Georgi, “*Softly broken supersymmetry and $SU(5)$* ”, Nucl. Phys. B **193**, 150 (1981).

- [184] S. Schael *et al.* (ALEPH, DELPHI, L3, OPAL and LEP Electroweak Collaborations), “*Electroweak measurements in electron-positron collisions at W -boson-pair energies at LEP*”, Phys. Rept. **532**, 119 (2013), <http://lepewwg.web.cern.ch/LEPEWWG>.
- [185] G. Aad *et al.* (ATLAS Collaboration), “*Observation of a new particle in the search for the Standard Model Higgs boson with the ATLAS detector at the LHC*”, Phys. Lett. B **716**, 1 (2012).
- [186] S. Chatrchyan *et al.* (CMS Collaboration), “*Observation of a new boson at a mass of 125 GeV with the CMS experiment at the LHC*”, Phys. Lett. B **716**, 30 (2012).
- [187] V. M. Abazov *et al.* (D0 Collaboration), “*Search for the Standard Model Higgs boson in the $t\bar{t}H \rightarrow t\bar{t}b\bar{b}$ channel*”, D0 Note 5739-CONF (2009).
- [188] T. Aaltonen *et al.* (CDF Collaboration), “*Search for the Higgs boson produced in association with top quarks*”, CDF Note 10801 (2012).
- [189] G. Aad *et al.* (ATLAS Collaboration), “*Search for the Standard Model Higgs boson produced in association with top quarks and decaying into $b\bar{b}$ in $p\bar{p}$ collisions at $\sqrt{s} = 8$ TeV with the ATLAS detector*”, Eur. Phys. J. C **75**, 349 (2015).
- [190] S. Chatrchyan *et al.* (CMS Collaboration), “*Search for a Standard Model Higgs boson produced in association with a top-quark pair and decaying to bottom quarks using a matrix element method*”, Eur. Phys. J. C **75**, 251 (2015).
- [191] T. Lee, “*A theory of spontaneous T violation*”, Phys. Rev. D **8** 1226 (1973).
- [192] V. M. Abazov *et al.* (D0 Collaboration), “*Search for charged Higgs bosons decaying into top and bottom quarks in $p\bar{p}$ collisions*”, Phys. Rev. Lett. **102**, 191802 (2009).
- [193] S. Chatrchyan *et al.* (CMS Collaboration), “*Search for a heavy charged Higgs boson in proton-proton collisions at $\sqrt{s} = 8$ TeV with the CMS detector*”, CMS-PAS-HIG-13-026 (2014).
- [194] T. Aaltonen *et al.* (CDF Collaboration), “*Search for charged Higgs bosons from top quark decays in $p\bar{p}$ collisions at $\sqrt{s} = 1.96$ TeV*”, Phys. Rev. Lett. **96**, 042003 (2006).
- [195] V. M. Abazov *et al.* (D0 Collaboration), “*Search for charged Higgs bosons in decays of top quarks*”, Phys. Rev. D **80**, 051107 (2009).

- [196] V. M. Abazov *et al.* (D0 Collaboration), “Combination of $t\bar{t}$ cross section measurements and constraints on the mass of the top quark and its decay into charged Higgs bosons”, Phys. Rev. D **80**, 071102 (2009).
- [197] G. Aad *et al.* (ATLAS Collaboration), “Search for charged Higgs bosons decaying via $H^\pm \rightarrow \tau^\pm \nu$ in fully hadronic final states using pp collision data at $\sqrt{s} = 8$ TeV with the ATLAS detector”, J. High Energy Phys. **1503**, 088 (2015).
- [198] S. Chatrchyan *et al.* (CMS Collaboration), “Search for charged Higgs bosons with the H^+ to $\tau\nu$ decay channel in the fully hadronic final state at $\sqrt{s} = 8$ TeV”, CMS-PAS-HIG-14-020 (2014).
- [199] T. Aaltonen *et al.* (CDF Collaboration), “Search for charged Higgs bosons in decays of top quarks in $p\bar{p}$ collisions at $\sqrt{s} = 1.96$ TeV”, Phys. Rev. Lett. **103**, 101803 (2009).
- [200] G. Aad *et al.* (ATLAS Collaboration), “Search for a light charged Higgs boson in the decay channel $H^+ \rightarrow c\bar{s}$ in $t\bar{t}$ events using pp collisions at $\sqrt{s} = 7$ TeV with the ATLAS detector”, Eur. Phys. J. C **73**, 2465 (2013).
- [201] S. Chatrchyan *et al.* (CMS Collaboration), “Search for H^+ to $c\bar{s}$ decay”, CMS-PAS-HIG-13-035 (2014).
- [202] V. M. Abazov *et al.* (D0 Collaboration), “Search for charged Higgs bosons in top quark decays”, Phys. Lett. B **682**, 278 (2009).
- [203] S. P. Martin, “A supersymmetry primer”, [arXiv:hep-ph/9709356v6](https://arxiv.org/abs/hep-ph/9709356v6) (2011).
- [204] T. Aaltonen *et al.* (CDF Collaboration), “Search for pair production of stop quarks mimicking top event signatures”, Phys. Rev. Lett. **104**, 251801 (2010).
- [205] G. Aad *et al.* (ATLAS Collaboration), “ATLAS Run 1 searches for direct pair production of third-generation squarks at the Large Hadron Collider”, Eur. Phys. J. C **75**, 510 (2015).
- [206] G. Aad *et al.* (ATLAS Collaboration), “Measurement of spin correlation in top-antitop quark events and search for top squark pair production in pp collisions at $\sqrt{s} = 8$ TeV using the ATLAS detector”, Phys. Rev. Lett. **114**, 142001 (2015).
- [207] S. Chatrchyan *et al.* (CMS Collaboration), “Search for top-squark pair production in the single lepton final state in pp collisions at 8 TeV”, Eur. Phys. J. C **73**, 2677 (2013).

- [208] S. Chatrchyan *et al.* (CMS Collaboration), “*Exclusion limits on gluino and top-squark pair production in natural SUSY scenarios with inclusive razor and exclusive single-lepton searches at 8 TeV*”, CMS-PAS-SUS-14-011 (2014).
- [209] S. Chatrchyan *et al.* (CMS Collaboration), “*Search for direct production of stops decaying to a charm and LSP using the monojet + MET final state*”, CMS-PAS-SUS-13-009 (2014).
- [210] S. Chatrchyan *et al.* (CMS Collaboration), “*Search for top squarks in multijet events with large missing momentum in pp collisions at 8 TeV*”, CMS-PAS-SUS-13-015 (2013).
- [211] V. Khachatryan *et al.* (CMS Collaboration), “*Searches for third-generation squark production in fully hadronic final states in proton-proton collisions at $\sqrt{s} = 8$ TeV*”, J. High Energy Phys. **1506**, 116 (2015).
- [212] G. Aad *et al.* (ATLAS Collaboration), “*Search for direct top squark pair production in events with a Z boson, b-jets and missing transverse momentum in $\sqrt{s} = 8$ TeV pp collisions with the ATLAS detector*”, Eur. Phys. J. C **74**, 2883 (2014).
- [213] V. Khachatryan *et al.* (CMS Collaboration), “*Search for top-squark pair production with Higgs and Z bosons in the final state in pp collisions at 8 TeV*”, Phys. Lett. B **736**, 371 (2014).
- [214] G. Aad *et al.* (ATLAS Collaboration), “*Search for strong production of supersymmetric particles in final states with missing transverse momentum and at least three b-jets at $\sqrt{s} = 8$ TeV proton-proton collisions with the ATLAS detector*”, J. High Energy Phys. **1410**, 024 (2014).
- [215] S. Chatrchyan *et al.* (CMS Collaboration), “*Search for supersymmetry using events with a single lepton, multiple jets, and b-tags*”, Phys. Lett. B **733**, 328 (2014).
- [216] D. B. Kaplan and H. Georgi, “*SU(2) X U(1) breaking by vacuum misalignment*”, Phys. Lett. B **136**, 183 (1984).
- [217] D. B. Kaplan, H. Georgi and S. Dimopoulos, “*Composite Higgs scalars*”, Phys. Lett. B **136**, 187 (1984).
- [218] H. Georgi and D. B. Kaplan, “*Composite Higgs and custodial SU(2)*”, Phys. Lett. B **145**, 216 (1984).
- [219] S. Weinberg, “*Approximate symmetries and pseudo-Goldstone bosons*”, Phys. Rev. Lett. **29** 1698 (1972).

- [220] H. Georgi and A. Pais, “*Calculability and naturalness in gauge theories*”, Phys. Rev. D **10**, 539 (1974).
- [221] H. Georgi and A. Pais, “*Vacuum symmetry and the pseudo-Goldstone phenomenon*”, Phys. Rev. D **12**, 508 (1975).
- [222] N. Arkani-Hamed, A. G. Cohen and H. Georgi, “*Electroweak symmetry breaking from dimensional deconstruction*”, Phys. Lett. B **513**, 232 (2001).
- [223] T. Aaltonen *et al.* (CDF Collaboration), “*Search for a heavy toplike quark in $p\bar{p}$ collisions at $\sqrt{s} = 1.96$ TeV*”, Phys. Rev. Lett. **107**, 261801 (2011).
- [224] V. M. Abazov *et al.* (D0 Collaboration), “*Search for a fourth generation t' quark in $p\bar{p}$ collisions at $\sqrt{s} = 1.96$ TeV*”, Phys. Rev. Lett. **107**, 082001 (2011).
- [225] T. Aaltonen *et al.* (CDF Collaboration), “*Search for heavy bottom-like quarks decaying to an electron or muon and jets in $p\bar{p}$ collisions at $\sqrt{s} = 1.96$ TeV*”, Phys. Rev. Lett. **106**, 141803 (2011).
- [226] G. Aad *et al.* (ATLAS Collaboration), “*Search for production of vector-like quark pairs and of four top quarks in the lepton plus jets final state in pp collisions at $\sqrt{s} = 8$ TeV with the ATLAS detector*”, ATLAS-CONF-2015-012 (2015).
- [227] G. Aad *et al.* (ATLAS Collaboration), “*Analysis of events with b -jets and a pair of leptons of the same charge in pp collisions at $\sqrt{s} = 8$ TeV with the ATLAS detector*”, J. High Energy Phys., **1510**, 150 (2015).
- [228] G. Aad *et al.* (ATLAS Collaboration), “*Search for pair and single production of new heavy quarks that decay to a Z boson and a third-generation quark in pp collisions at $\sqrt{s} = 8$ TeV with the ATLAS detector*”, J. High Energy Phys. **1411**, 104 (2014).
- [229] V. Khachatryan *et al.* (CMS Collaboration), “*Inclusive search for a vector-like T quark with charge $2/3$ in pp collisions at $\sqrt{s} = 8$ TeV*”, Phys. Lett. B **729**, 149 (2014).
- [230] S. Chatrchyan *et al.* (CMS Collaboration), “*Search for pair-produced vector-like quarks of charge $-1/3$ in lepton + jets final state in pp collisions at $\sqrt{s} = 8$ TeV*”, CMS-PAS-B2G-12-019 (2013).
- [231] V. Khachatryan *et al.* (CMS Collaboration), “*Search for top quark partners with kinematic reconstruction in single-lepton final states*”, CMS-PAS-B2G-12-017 (2014).

- [232] V. Khachatryan *et al.* (CMS Collaboration), “Search for vector-like T quarks decaying to top quarks and Higgs bosons in the all-hadronic channel using jet substructure”, *J. of High Energy Phys.* **1506**, 080 (2015).
- [233] V. Khachatryan *et al.* (CMS Collaboration), “Search for the production VLQ $T' \rightarrow tH$, $H \rightarrow \gamma\gamma$ ”, CMS-PAS-B2G-14-003 (2014).
- [234] G. Aad *et al.* (ATLAS Collaboration), “Search for vector-like B quarks in events with one isolated lepton, missing transverse momentum and jets at $\sqrt{s} = 8$ TeV with the ATLAS detector”, *Phys. Rev. D* **91**, 112011 (2015).
- [235] N. Arkani-Hamed, S. Dimopoulos, and G. R. Dvali, “The hierarchy problem and new dimensions at a millimeter”, *Phys. Lett. B* **429**, 263 (1998).
- [236] L. Randall and R. Sundrum, “A large mass hierarchy from a small extra dimension”, *Phys. Rev. Lett.* **83**, 3370 (1999).
- [237] L. Randall and R. Sundrum, “An alternative to compactification”, *Phys. Rev. Lett.* **83**, 4690 (1999).
- [238] V. M. Abazov *et al.* (D0 Collaboration), “Search for $W' \rightarrow tb$ resonances with left- and right-handed couplings to fermions”, *Phys. Lett. B* **699**, 145 (2011).
- [239] T. Aaltonen *et al.* (CDF Collaboration), “Search for resonances decaying to top and bottom quarks with the CDF experiment”, *Phys. Rev. Lett.* **115**, 061801 (2015).
- [240] G. Aad *et al.* (ATLAS Collaboration), “Search for $W' \rightarrow tb$ in the lepton plus jets final state in proton-proton collisions at a centre-of-mass energy of $\sqrt{s} = 8$ TeV with the ATLAS detector”, *Phys. Lett. B* **743**, 235 (2015).
- [241] S. Chatrchyan *et al.* (CMS Collaboration), “Search for W' to tb decays in the lepton + jets final state in pp collisions at $\sqrt{s} = 8$ TeV”, *J. High Energy Phys.* **1405**, 108 (2014).
- [242] R. M. Harris, C. T. Hill, and S. J. Parke, “Cross section for topcolor Z' decaying to top-antitop”, [arXiv:hep-ph/9911288](https://arxiv.org/abs/hep-ph/9911288) (1999).
- [243] V. M. Abazov *et al.* (D0 Collaboration), “Search for a narrow $t\bar{t}$ resonance in $p\bar{p}$ collisions at $\sqrt{s} = 1.96$ TeV”, *Phys. Rev. D* **85**, 051101(R) (2012).
- [244] J. M. Butterworth, A. R. Davison, M. Rubin, G. P. Salam, “Jet substructure as a new Higgs search channel at the LHC”, *Phys. Rev. Lett.* **100**, 242001 (2008).

- [245] G. Aad *et al.* (ATLAS Collaboration), “A search for $t\bar{t}$ resonances using lepton-plus-jets events in proton-proton collisions at $\sqrt{s} = 8$ TeV with the ATLAS detector”, J. High Energy Phys., **1508**, 148 (2015).
- [246] S. Chatrchyan *et al.* (CMS Collaboration), “Search for resonant $t\bar{t}$ production in proton-proton collisions at $\sqrt{s} = 8$ TeV”, subm. to Phys. Rev. D, [arXiv:1506.03062 \[hep-ex\]](https://arxiv.org/abs/1506.03062) (2015).
- [247] C. Quigg, “Top-ology”, Proceedings of the LAFEX International School of High Energy Physics, Workshop on Heavy Flavors, *cbt*, Rio de Janeiro, February 1995, [arXiv:hep-ph/9507257](https://arxiv.org/abs/hep-ph/9507257) (1995).